

Comparison of metal-poor stars in the Milky Way halo and in  
the dwarf spheroidal galaxy Sculptor, with emphasis on Carbon  
Enhanced Metal-Poor stars

Bachelor Research Report  
Kapteyn Institute Groningen

Anke Arentsen  
Supervisor: Eline Tolstoy

July 9, 2014



**kapteyn astronomical  
institute**

## Abstract

In this study, we compare the properties of metal-poor stars in the Milky Way halo and in the dwarf spheroidal (dSph) galaxy Sculptor. Metal-poor stars are interesting because they carry the imprints of the early chemical evolution in galaxies. The metal-poor stars in the halo and Sculptor should have similar properties because they both belong to very old systems that are thought to have a common origin. In the halo, Carbon Enhanced Metal-Poor (CEMP) stars are found in great number among the lowest metallicity stars. These stars with a lot of carbon are barely found in dwarf spheroidal systems like Sculptor. We compare the halo and Sculptor making use of the Hertzsprung-Russell diagram. We also carry out statistics on the possibility that the CEMP fraction with metallicity in the halo is different from Sculptor, assuming 1 identified CEMP and 9 CEMP candidate stars in Sculptor. The result is that the fractions could be the same, but it is a conclusion from very small number statistics and not highly significant. The research on CEMP stars in Sculptor should continue, so that more can be discovered about differences or similarities between the halo and Sculptor.

# Contents

<b>1</b>	<b>Introduction</b>	<b>3</b>
1.1	The halo . . . . .	3
1.2	Sculptor . . . . .	4
1.3	Metal-poor stars . . . . .	4
1.4	Carbon Enhanced Metal-Poor stars . . . . .	5
<b>2</b>	<b>Observations</b>	<b>7</b>
2.1	Halo sample . . . . .	7
2.1.1	Working with the data table . . . . .	8
2.1.2	Effective temperature and surface gravity . . . . .	8
2.2	Sculptor sample . . . . .	9
2.2.1	High resolution . . . . .	10
2.2.2	Low resolution . . . . .	11
2.2.3	Extra stars added to the Sculptor sample . . . . .	11
<b>3</b>	<b>Comparing the two samples</b>	<b>12</b>
3.1	Abundances . . . . .	12
3.1.1	Metallicity . . . . .	12
3.1.2	Alpha elements . . . . .	13
3.2	HR diagram . . . . .	14
3.2.1	Metallicity dependence . . . . .	16
<b>4</b>	<b>CEMP stars</b>	<b>17</b>
4.1	CEMP stars in the halo . . . . .	17
4.2	CEMP stars in Sculptor . . . . .	22
4.2.1	Ása's star . . . . .	22
4.2.2	More CEMP candidates . . . . .	22
4.3	Some statistics . . . . .	23
4.4	Conclusions . . . . .	24
	<b>Summary and Discussion</b>	<b>25</b>
	<b>References</b>	<b>27</b>
	<b>Appendix</b>	<b>28</b>

# Chapter 1

## Introduction

There is a general consensus that galaxies like the Milky Way must have been formed by multiple mergers of smaller galaxies, a process called hierarchical galaxy formation. Some of this type of dwarf galaxies are still present in the proximity of the Milky Way. If the Milky Way has been formed out of these small galaxies long ago, the oldest stars in both systems should have similar properties. The oldest stars are likely to be the most metal-poor, since chemical enrichment of the interstellar medium can only build up with time. So to be able to draw conclusions about whether or not the Milky Way can be formed from dwarf galaxies like those around it, we should compare the most metal-poor stars in both the Milky Way and the dwarf galaxies. In this study we compare a sample of stars from the Milky Way stellar halo with a sample in the dwarf spheroidal (dSph) galaxy Sculptor.

### 1.1 The halo

The Milky Way consists of several components, the thin disk, the thick disk, the bulge and the halo. See Figure 1.1 for a schematic view of the Milky Way. The thin disk mainly consists of young stars, because there is a lot of star formation there. The thick disk is more diffuse and has stars which are older. Both disks are rotating. The bulge mainly consists of old, metal-rich stars. There is a very small younger population in the bulge and a bit of star formation

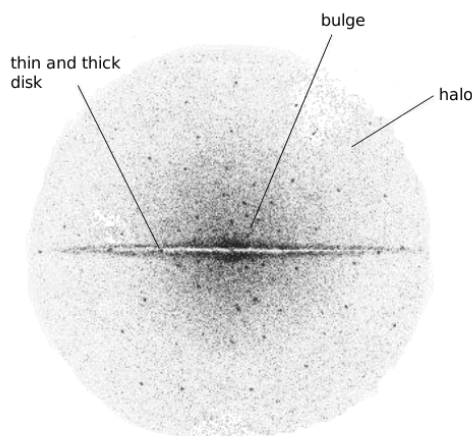


Figure 1.1 *Schematic view of the Milky Way (from: see references)*

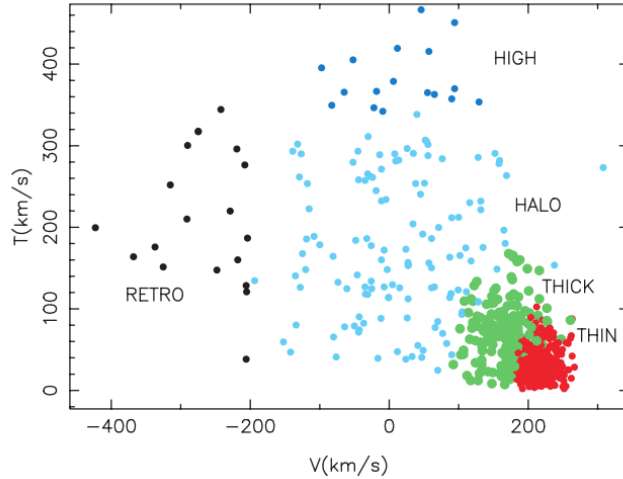


Figure 1.2 *Decomposition of the Milky Way into components using kinematics in the  $U, V, W$  system.  $V$  is the velocity in the direction of rotation,  $T = \sqrt{U^2 + W^2}$  which is a measure of the random motion. Figure from Venn et al. (2004).*

(Wyse & Gilmore, 2005). The halo is very diffuse and as a whole it is not rotating like the thick and thin disks. There is currently no star formation in the halo and it consists mostly of the oldest and most metal-poor stars in the Milky Way. The halo is thought to be the most ancient component of the Milky Way. It is certainly where the most metal-poor stars are found.

The components of the Milky Way can be distinguished in several ways. The main way to distinguish them is kinematically. Stars from every component are moving in specific ways. The velocities of the stars in different directions determines for the component they belong to. Stars that have velocities mainly in the direction of rotation of the galaxy and not in other directions are likely to be part of the thin disk. If there is also some velocity perpendicular to the direction of rotation, the star might be a thick disk star. Halo stars have velocities in almost completely random directions. This decomposition is shown in Figure 1.2.

## 1.2 Sculptor

Sculptor is a dwarf spheroidal galaxy that has been extensively studied. It is a satellite of the Milky Way, at a distance of  $86 \pm 5$  kpc (Pietrzyński et al. 2008), well inside the Local Group. It had a peak in star formation  $\sim 12$  Gyr ago and it stopped forming stars  $\sim 7$  Gyr ago (de Boer et al. 2012), so it contains mostly old stars. This makes it a good candidate to study early star formation and chemical enrichment processes.

## 1.3 Metal-poor stars

Before continuing, it is useful to define the concept of metallicity. Metallicity is usually given as the abundance of iron with respect to hydrogen. It is written as  $[\text{Fe}/\text{H}]$ , which is defined with respect to the Sun as  $\log(\text{Fe}/\text{H})_* - \log(\text{Fe}/\text{H})_\odot$ , where the  $*$  denotes the star we are interested in and  $\odot$  indicates the solar value. Abundances for other elements can be written in the same way. A star is metal-poor according to Beers & Christlieb (2005) if it has  $[\text{Fe}/\text{H}] < -1.0$ , very metal-poor if it has  $[\text{Fe}/\text{H}] < -2.0$  and extremely metal-poor if it has  $[\text{Fe}/\text{H}] < -3.0$ . Whenever

the word metallicity is used in this study, we refer to  $[\text{Fe}/\text{H}]$ . Although  $[\text{Fe}/\text{H}]$  is used to define the metallicity, it does not necessarily refer to the total amount of metals in a star. If a star is very iron-poor it can still have a high abundance in other elements.

The first large survey for metal-poor stars in the Milky Way was the HK survey (Beers et al. 1985, 1992). A more recent survey is the Hamburg/ESO (HES) survey for metal-poor stars (Christlieb et al. 2008). From these surveys, candidate metal-poor stars can be selected from the low resolution spectroscopy on the basis of the strength of their CaII H and K lines. These candidates can be followed up with higher resolution spectroscopy. There is also a project that makes use of the SDSS to find more metal-poor stars, the Sloan Extension for Galactic Understanding and Exploration (SEGUE) (Yanny et al. 2009). Many metal-poor stars have been found in the halo because of these and other surveys, and still more are being found today.

A way to find metal-poor stars in a galaxy like Sculptor dSph is to carry out a low resolution Calcium Triplet (CaT) spectroscopic survey and follow up candidate metal-poor stars with higher resolution spectroscopy. Candidates are chosen by looking at the strength of the three CaT lines that are among the strongest spectral features in the optical range. The weaker these lines are, the lower  $[\text{Fe}/\text{H}]$  of a star. The most interesting stars are followed up with high resolution spectroscopy. From those spectra, abundances of many elements can be measured.

## 1.4 Carbon Enhanced Metal-Poor stars

It was noticed in the HK survey that many metal-poor stars in the halo have unusually strong CH G bands, which indicates a high carbon abundance. It seemed like many of these metal-poor stars had much more carbon than initially expected. This apparent large fraction of Carbon Enhanced Metal-Poor (CEMP) stars has been confirmed later by the HES survey. The original definition for CEMP stars was the one of Beers & Christlieb (2005), which states that all stars with  $[\text{Fe}/\text{H}] \leq -2.0$  and  $[\text{C}/\text{Fe}] \geq +1.0$  are CEMP stars. The definition of CEMP stars used in this study is a more recent one from Aoki et al. (2007), which takes nucleosynthesis and mixing in evolved giants into account. These are processes which can influence the carbon abundance measured in stars. In evolved giant stars, convective layers start developing and they bring material from the inside of the star to the surface, where it mixes with the surface elements. This process can decrease the amount of carbon on the surface of a star. This means that a CEMP star earlier in its lifetime will have a higher carbon abundance than we see today. The same CEMP star could be overlooked if it is in a more evolved state, if the definition would not take the mixing effect into account. This dependence has been expressed in terms of luminosity.

Stars that satisfy the following criteria are considered CEMP stars according to the Aoki et al. (2007) definition:

$$\begin{array}{ll} [\text{C}/\text{Fe}] \geq +0.7 & \text{for stars with } \log(L/L_{\odot}) \leq 2.3 \\ [\text{C}/\text{Fe}] \geq +3.0 - \log(L/L_{\odot}) & \text{for stars with } \log(L/L_{\odot}) > 2.3 \end{array}$$

It has been noticed that the fraction CEMP stars in the halo increases with decreasing  $[\text{Fe}/\text{H}]$ . The CEMP fraction rises up to more than 30% for stars with  $[\text{Fe}/\text{H}] < -3.0$  (Beers & Christlieb 2005, Lee et al. 2013). This suggests that large amounts of carbon (compared to iron) were somehow produced early in the universe, when the oldest and most metal-poor stars were created.

To be able to understand where they come from, CEMP stars should be investigated. Different types of CEMP stars are found, and they can be sub-classified as CEMP-r, CEMP-s, CEMP-r/s or CEMP-no. The r stands for the rapid neutron capture process and the s for the slow neutron capture process. Signatures of these processes can be found in CEMP-r, CEMP-s and CEMP-r/s stars. The rapid process occurs mainly in supernova events, while the slow process usually happens in stars during or towards the end of their lifetime. It is not clear how CEMP-r and CEMP-r/s stars are formed.

For the CEMP-s stars, it is quite well-known how they are formed (Lucattello et al. 2005). Carbon can be produced by an intermediate mass star in its AGB stage and then transferred to a lower mass companion star. These companion stars can be identified as CEMP-s stars, because besides enhancement in carbon they also show enhancement in s-process elements (and not in r-process elements). These s-process elements have been created by the intermediate mass AGB star and transferred to the (what is now a) CEMP star. This type of CEMP star is always part of a binary system. Measurements of radial velocities of stars can point out whether they are part of a binary or not.

There is also a type of CEMP star which is called a CEMP-no star, because it does not show any signatures of enhancement in r- or s-process elements. These are the most interesting CEMP stars, since there is not yet a well-known mechanism that can produce them. According to Aoki (2010)  $\sim 90\%$  of the stars below  $[\text{Fe}/\text{H}] = -3.0$  belong to the CEMP-no subclass. It is thought that the carbon abundance in these CEMP-no stars is (close to) primordial, contrary to the carbon in the previous subclasses. It might be that there is an intrinsic mechanism in the most metal-poor stars for creating carbon very efficiently and depositing it on the surface. Another possibility is that their element content might be the product of many faint supernovae (from stars with a maximum mass of  $\sim 12 M_{\odot}$ ) in the early universe (Aoki 2010). The CEMP-no stars have formed from the interstellar medium resulting from these faint supernovae. This is for now probably the most likely explanation.

It might be good to note here that there also exist stars which are called carbon stars, but they are something else than CEMP stars. In these carbon stars, the carbon abundance with respect to oxygen goes up as a result of mixing very late in the evolution of a star. This is a well known evolutionary effect and has nothing to do with the extra high carbon abundances in the CEMP stars we are looking at.

If the chemical composition of the Milky Way halo is similar to that in Sculptor, we should expect to see these CEMP stars in Sculptor as well since the CEMP fraction in the halo is quite high. But only one CEMP star has been found in Sculptor very recently (Skúladóttir et al. in prep.), with  $[\text{Fe}/\text{H}] = -2.03$ . In this study, we want to understand why CEMP stars are not found as frequently in Sculptor as in the halo, despite extensive searches of the metal-poor population. To achieve this, we will specifically look at the effective temperatures and surface gravities of the most metal-poor stars in the halo and in Sculptor. These two parameters can be plotted against each other in a Hertzsprung-Russel diagram (HR diagram) type plot. From this diagram we can learn about the phases of stellar evolution. We will compare the Sculptor and halo stars in location on this diagram, to see how they are different and if this is a reason that not more CEMP stars are found in Sculptor. We will also take into account a possible dependence on metallicity.

In Chapter 2 we will describe the samples of stars that we use in this work. In Chapter 3 we will compare some properties of these samples and in Chapter 4 we will specifically discuss CEMP stars in the halo and in Sculptor.

## Chapter 2

# Observations

In order to be able to investigate differences between the Milky Way halo and Sculptor, large uniform samples of metal-poor stars are needed for both galaxies. We used one uniform sample with very to extremely metal-poor stars for the halo and we used one large sample for Sculptor which is overall less metal-poor. This sample is divided into two samples based on the resolution of the available spectroscopy. In this chapter we will describe these samples.

### 2.1 Halo sample

We used a uniformly analyzed sample of metal-poor stars in the halo of the Milky Way from Yong et al. (2013a). They present tables with stellar parameters and several measured abundances for 190 stars, of which 171 have  $[\text{Fe}/\text{H}] < -2.5$ . This very metal-poor sample is not a representative sample for the entire halo, only for the very low metallicity part. In An et al. 2012 the metallicity distribution function for the halo has been described. In Figure 2.1 we show a part of their Figure 18 where the metallicity distribution function is plotted. From this figure it is clear that by only looking at stars with metallicities mostly lower than  $-2.5$ , Yong et al. are only looking at the tail of the distribution.

Yong et al. present their own program sample of 38 stars, and took 152 stars from the literature. Stars from the literature were chosen from the SAGA database (Suga et al. 2008). For every star they present values for the effective temperatures ( $T_{eff}$ ), surface gravities ( $\log g$ ),  $[\text{Fe}/\text{H}]$  and whether the star is a CEMP star or not (according to the Aoki et al. (2007) definition). Where possible, element to iron ratios for C, N, Na, Mg, Al, Si, Ca, Sc, Ti (I and II), Cr, Mn, FeII, Co, Ni, Sr and Ba were presented.

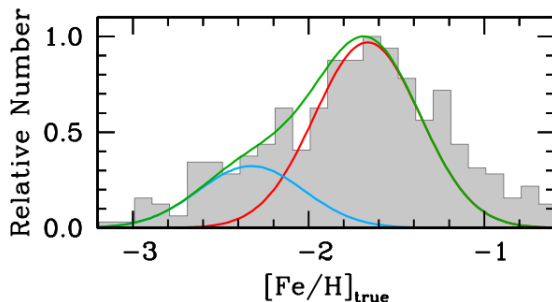


Figure 2.1 *The gray histogram shows the normalized observed  $[\text{Fe}/\text{H}]$  distribution in the Milky Way halo. The curves are modeling this distribution. From An et al. (2012)*

### 2.1.1 Working with the data table

It was not easy at first to work with the table for the data from this sample. From the online paper a text file of the table could be obtained, but Python cannot simply read such a table if there are gaps in it, which was the case for this table since not for every star all the abundances were given. It has taken some time and a lot of trying to find a good way to read tables like this. In the end the method we used was importing the text file into *LibreOffice Calc*, setting columns by hand and then exporting to a .csv (comma separated value) file. This worked because in this file the gaps in the table could be read as empty. This made it also a lot easier to edit the table or to add columns, because *LibreOffice Calc* is a nice environment to work with tables. This method of importing tables has been used for all tables in this study.

### 2.1.2 Effective temperature and surface gravity

We are interested in the location of stars on the HR diagram, because it tells us something about the evolutionary stage of stars. On an HR diagram, theoretical lines can be plotted for systems with a certain age, alpha element content and metallicity. These lines of stars of the same age are called isochrones. The parameters we use for the HR diagram are effective temperature and surface gravity. In Norris et al. (2013) the  $T_{eff}$  and  $\log g$  were determined for the Yong et al. halo sample. This has been done differently for the program stars and the literature stars. For the program stars, they used three different methods to derive effective temperatures. The methods were fitting of model atmosphere fluxes to spectrophotometric observations; derivation from hydrogen  $\alpha$ ,  $\beta$  and  $\gamma$  line profiles; and thirdly from the hydrogen  $\delta$ -line index. This is all mainly from spectroscopy, not photometry. The  $\log g$  then is determined from fitting the  $T_{eff}$  to Y2 isochrones from Demarque et al. (2004).

For the literature sample Yong et al. could not do the rigorous derivation of effective temperature that was used for their program stars, because the necessary information was not available for all stars. Only for a subset of the literature sample could  $T_{eff}$  be calculated in the same way. For stars for which they could not make the same  $T_{eff}$  derivation, they used the infrared flux method (IRFM). This is a method in which a metallicity-dependent color-temperature relation is used to find  $T_{eff}$ . This means that the effective temperatures were calculated from photometry, not from spectroscopy as before. For the IRFM they adopted a relation from Casagrande et al. (2010) for the dwarfs and a relation for the giants from Ramírez & Meléndez (2005). The  $\log g$  was determined in the same way as before.

It has been shown in Norris et al. (2013) that equivalent width measurements used in calculating  $\log g$  for their program sample are on the same scale as in various literature studies. This means that the  $\log g$  for the two samples are determined in a similar way with similar results. Also the  $T_{eff}$  values for the IRFM and for the program stars have been carefully compared and made uniform. We assume that the program and literature samples together can safely be considered as one uniform sample.

## 2.2 Sculptor sample

The spectroscopy of individual stars in Sculptor dSph came from the Dwarf Abundances and Radial velocities Team (DART) survey (Tolstoy et al. 2006). This survey consists of a large sample for which low resolution calcium triplet (CaT) spectroscopy is presented (Battaglia et al. 2008) and a high resolution detailed abundance determination for a smaller sample (Hill et al. in prep.). From CaT spectroscopy, an estimate for  $[\text{Fe}/\text{H}]$  can be determined. Tolstoy et al. 2006 present photometry in the V and I bands and estimates for  $[\text{Fe}/\text{H}]$  for  $\sim 1500$  stars. This is our low resolution (LR) sample. From this large sample, a subset of stars has been targeted for follow up with high resolution (HR) spectroscopy. This is our HR sample. For many of the stars in this HR sample J and  $K_S$  band photometry is also available.

For the LR and HR samples, effective temperatures and surface gravities have to be derived from the photometry. The method used for calculating  $T_{eff}$  is the infrared flux method (IRFM). We will use this method later but we will explain it now. For giants (which all the stars in the Sculptor spectroscopic samples are), the color and metallicity dependent temperature calibrations can be taken from Ramírez and Meléndez (2005). The conversion from color and metallicity to effective temperature goes as follows:

$$\theta_{eff} = a_0 + a_1X + a_2X^2 + a_3X[\text{Fe}/\text{H}] + a_4[\text{Fe}/\text{H}] + a_5[\text{Fe}/\text{H}]^2, \quad (2.1)$$

$$T_{eff} = \frac{5040}{\theta_{eff}} + \sum_i P_i X^i, \quad (2.2)$$

where X is the color. Values for  $a_0$  to  $a_5$  and the values for  $P_i$  can be taken from Tables 3 and 5 respectively from Ramírez and Meléndez (2005). These values are different for different colors and metallicity ranges. This conversion is only applicable to stars that fall inside specific color ranges (which are again also dependent on  $[\text{Fe}/\text{H}]$ ), as indicated in Table 5 in Ramírez and Meléndez (2005). If stars fall outside these ranges, no good calculation of  $T_{eff}$  can be made.

The values for  $\log g$  can be derived from the temperatures using the following relation:

$$\log(g) = \log(g_\odot) + \log(M/M_\odot) + 4\log(T/T_\odot) + 0.4(M_{bol} - M_{\odot,bol}), \quad (2.3)$$

where we assume  $g_\odot = 4.44$ ,  $T_\odot = 5790\text{K}$ , the solar bolometric magnitude  $M_{\odot,bol} = 4.72$  and a mass of  $M = 0.8M_\odot$ . This mass comes from the average age of stars in Sculptor. For calculating  $M_{bol}$ , the distance modulus to Sculptor needs to be known and the bolometric correction (BC) has to be calculated. The distance modulus we adopt is 19.54 from Tolstoy et al. (2003). The BC for the V band can be calculated using Equations 17 and 18 from Alonso et al. (1999). The conversion is only valid for specific ranges in effective temperature and  $[\text{Fe}/\text{H}]$ . These ranges can be found in their Equations 17 and 18 as well. If stars fall outside the ranges, no good derivation of  $\log g$  can be made. Using the V band magnitude in calculating the bolometric magnitude,  $M_{bol} = V - 19.54 + \text{BC}(V)$ , values for  $\log g$  can be obtained by filling in the obtained numbers in Equation 2.3.

### 2.2.1 High resolution

First we will look at the HR sample. Hill et al. (in prep.) present for the first time HR spectroscopy of a large number (99) stars in Sculptor. These results were also presented in Tolstoy et al. 2009. HR spectroscopy of stars outside our own galaxy used to be difficult, and could only be done one star at a time. For every star,  $\sim 5$  hours of observing was needed. This is not a very effective way to get data for a large sample of stars. But over the past few years it became possible to obtain spectroscopy of large samples thanks to multifiber facilities at for example FLAMES at the VLT. Hill et al. present HR spectroscopy of a sample of 99 giant stars on the upper red giant branch (RGB) which were selected from the LR CaT spectroscopy. Only HR spectroscopy of stars on the upper RGB could be done because they are the brightest stars and give the highest signal to noise most efficiently. See Figure 2.2 for the distribution of the randomly selected stars on the Sculptor RGB. The metallicity range in the sample roughly covers  $-2.5 < [\text{Fe}/\text{H}] < -1.0$ . For all of these stars  $T_{\text{eff}}$ ,  $\log g$  and  $[\text{Fe}/\text{H}]$  were determined. Where possible abundances of Na, O, Mg, Si, Ca, Ti (I and II), FeII, Sc, Cr, Mn, Ni, Co, Y, Ba, La, Nd and Eu are given. All these values can be found in Hill et al. (in prep.) The stars from the HR sample have been removed from the LR sample to avoid using the same star twice in this study.

The  $T_{\text{eff}}$  for all the stars has been determined in Hill et al. from photometry using the IRFM. For many of the stars in this HR sample, J and  $K_S$  band photometry was also available besides V and I. In Hill et al. in prep they calculated  $T_{\text{eff}}$  using three different colors: (V-I), (V-J) and (V- $K_S$ ). It turned out that the temperatures derived from (V-I) were on average 200K hotter than from the other two colors. They could not find a good reason why this was, so they averaged the three derived temperatures. For stars for which they only had (V-I) colors, they lowered  $T_{\text{eff}}$  by 130K so that all their stars are on the same temperature scale.

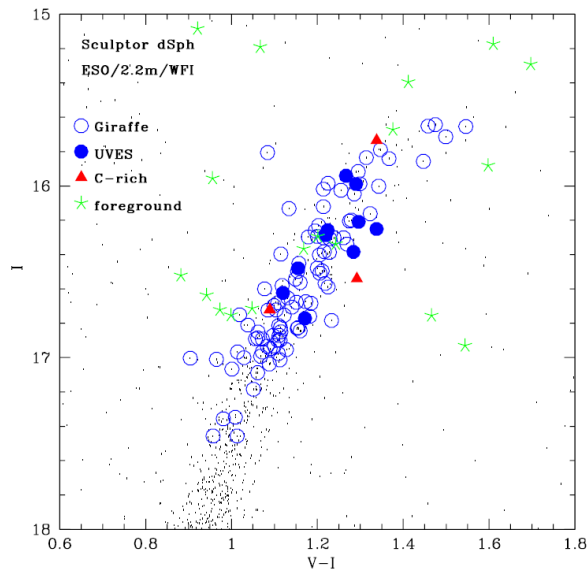


Figure 2.2 CMD of the tip of the RGB in Sculptor. Blue circles are the selected stars for which spectroscopy has been obtained. For the C-rich stars (red triangles), spectroscopy could not be obtained. Green stars indicate foreground stars. From Hill et al. (in prep.)

### 2.2.2 Low resolution

There are still many stars in the sample from DART that do not have high resolution spectroscopy, and they are our LR sample. For this sample, an estimate for  $[\text{Fe}/\text{H}]$  and photometry in the V and I bands was available. The  $T_{eff}$  in this sample can be determined with the IRFM, using photometry in the V and I bands. This has not been done before, so we did this ourselves. Before using the color (V-I), a reddening correction needs to be applied because there is some extinction in the direction of Sculptor. For Sculptor this reddening for the (V-I) color is  $E(V - I) = 0.023$  (Schlegel et al. 1998). The corrected color (V-I) now can be converted to effective temperature using Equations 2.1 and 2.2. For (V-I), only a value for  $P_0$  is given, and it is very small. The errors on the temperature are much bigger, so we ignore the P term here. We use the constants  $a_0 = 0.3575, a_1 = 0.9069, a_2 = -0.2025, a_3 = 0.0395, a_4 = -0.0551$  and  $a_5 = -0.0061$  for (V-I) from Table 3 from Ramírez and Meléndez (2005). Equation 2.1 with these constants only holds for certain metallicity and color ranges, which are given in Table 5 in that paper. They have been taken into account in deriving the temperatures for our data set. Since we only have (V-I) photometry for this LR sample, we lowered all our derived temperatures by 130K to be on the same scale as in the HR sample. Values for  $\log g$  were determined from  $T_{eff}$  using Equation 2.3 and calculating the bolometric correction from the V band magnitude.

There are 809 stars left from the 1500, the rest of the stars fell outside the applicable ranges somewhere in the derivation of  $T_{eff}$  or  $\log g$ . To be sure that the calculations we made are correct, we did not include the stars outside the ranges. Results for  $[\text{Fe}/\text{H}]$ ,  $T_{eff}$  and  $\log g$  including all corrections are given in Table 4.1 in the Appendix.

### 2.2.3 Extra stars added to the Sculptor sample

To this large uniform sample, we added 10 very to extremely metal-poor stars in Sculptor that high resolution spectroscopy was already available for in the literature. We do this to increase our range in metallicity, since we wanted to look at the most metal-poor stars. We took two stars from Tafelmeyer et al. (2010), with  $[\text{Fe}/\text{H}]$  of -3.48 and -3.96. We took one star from Frebel et al. (2010), which has  $[\text{Fe}/\text{H}] = -3.81$ . We also added seven stars from Starkenburg et al. (2010) with medium resolution (MR) spectroscopy, where  $[\text{Fe}/\text{H}]$  ranges from -2.46 to -3.47.

We will refer to all the stars from the HR, LR and extra samples together as the Sculptor sample.

## Chapter 3

# Comparing the two samples

Now that we have introduced the halo and Sculptor samples, we will look at them in a bit more detail. We will describe and compare some of their properties. This is a useful thing to do because it shows how the halo and Sculptor are similar and/or different. The results from this chapter can be taken into account when comparing CEMP fractions in the halo and Sculptor, which is the purpose of this study.

### 3.1 Abundances

For the stars with high resolution spectroscopy much is known about the stars in our samples in terms of chemical content. We picked two interesting (sets of) abundances to look at: the iron-abundance (or metallicity), and the alpha elements. We do this because they are interesting from a theoretical point of view, but also because it allows us to describe our samples better.

#### 3.1.1 Metallicity

We define the metallicity as  $[Fe/H]$ . The Sculptor sample as a whole is more metal-rich than the halo Yong et al. sample, see Figure 3.1 for the distribution in  $[Fe/H]$  of the stars in our samples.

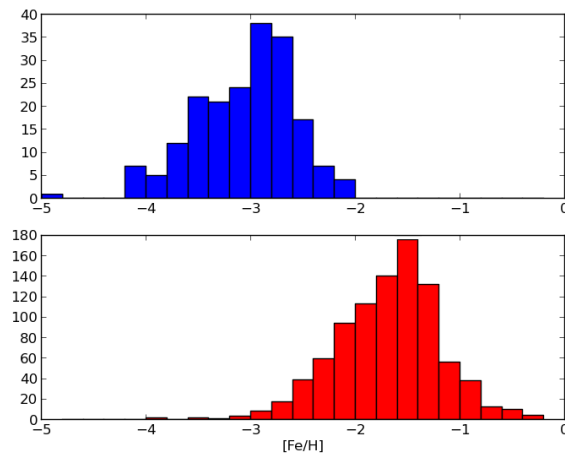


Figure 3.1 *Distribution of the number of stars per  $[Fe/H]$  in the halo Yong et al. sample (upper panel) and the Sculptor sample (lower panel). Note that the two panels do not have the same scale, there are many more stars in the Sculptor sample.*

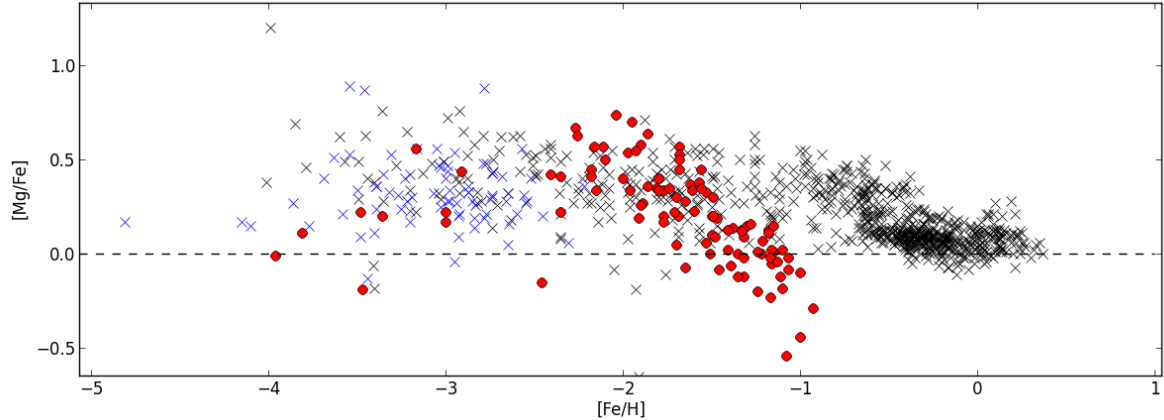


Figure 3.2 *Abundance of the alpha element Mg with respect to iron as a function of metallicity  $[Fe/H]$ . Blue crosses are the metal poor halo sample from Yong et al. (2013) black crosses are Milky Way stars from a uniform sample from Venn et al. (2004) and red circles are Sculptor stars*

Ofcourse the sample of the halo has specifically been chosen to be very metal-poor, there are higher metallicity stars present in the halo, but they are not in this sample. We use the Yong et al. sample because it is a uniformly analyzed metal-poor sample and because information about CEMP stars is available. For the Sculptor sample the distribution of  $[Fe/H]$  is thought to be a representative sample for the whole galaxy. There are some extremely metal-poor stars in the Sculptor sample, but very few. This seems surprising, because if dSph's like Sculptor are the building blocks of the Milky Way, why are there many extremely metal-poor stars in the halo but not in Sculptor? These are supposed to be the oldest stars and should be found in both systems. And it is not just in Sculptor, Helmi et al. (2006) observe the same in three other dSph's. They describe this problem as a kind of "G-dwarf problem" on the scale of the dSph's: some stars that you expect to be there are not found. However, quantifying this is challenging because comparing a tiny well-studied galaxy like Sculptor with the huge halo is non-trivial. The conclusion is that the distributions in metallicity are different, but we can try to compare stars that have similar metallicities, which restricts us to a range of more or less  $-3.0 < [Fe/H] < -2.0$ , the range of the very metal-poor stars.

### 3.1.2 Alpha elements

Besides iron, abundances for many other elements, like alpha elements, are available for the Yong et al. halo sample and the HR Sculptor sample. Alpha elements like Mg, Ca and Ti are created by the fusion of alpha particles (helium nuclei), and they are typically created in massive stars. This type of stars will explode in a SN Type II event, which occurs already very early in the universe since these heavy stars have very short lifetimes. The next generation of stars will have a certain level of alpha elements in them. The alpha abundance  $[\alpha/Fe]$  is at more or less a constant value for all the lowest metallicity stars, in Sculptor and the halo. At some point in the evolution of a galaxy, SN Type Ia will start to go off. These start later in time than SN type II because the progenitors for this type of SN (white dwarfs) take more time to evolve from low mass stars. These SN Type Ia produce a lot of Fe (much more than SN type II), and they release very little alpha elements with respect to iron because alpha elements are not created much inside low mass stars. So there is a time difference between the onset of the two

types of supernovae. As a result of this, at the time of the onset of SN type Ia, there is a change in  $[\alpha/\text{Fe}]$  in the galaxy, it goes down while  $[\text{Fe}/\text{H}]$  goes up. Metallicity and age are related, so saying that this happens at some point in time is likely similar to saying that it happens at a certain metallicity. This can be seen in Figure 3.2 for  $[\text{Mg}/\text{Fe}]$  (one of the alpha elements) for the Milky Way and Sculptor. The point where  $[\alpha/\text{Fe}]$  starts to go down is called the knee. The knee in this Figure is around  $[\text{Fe}/\text{H}] \approx -1.0$  for the Milky Way and around  $[\text{Fe}/\text{H}] \approx -2.0$  for Sculptor. The difference in location of the knee is also visible in other alpha elements. It means that the halo has been enriched to higher  $[\text{Fe}/\text{H}]$  than Sculptor before SN type Ia started playing a role. It is thought that the onset of SN type Ia takes about 1 Gyr, and if that is the same for Sculptor and the halo (and there is no good reason to assume a difference) that would mean that the different  $[\text{Fe}/\text{H}]$  of the knees would correspond to similar timescales. In the same time frame, the halo has been enriched in iron further than Sculptor. This is a clear difference in the evolution of both galaxies. It is good to keep in mind the fact that we already know that there are some differences between the halo and Sculptor, so we should be careful with the assumption that they are similar systems.

## 3.2 HR diagram

Besides comparing chemical content, we can also compare some physical parameters of stars. In Figure 3.3 the halo and Sculptor samples are shown on an HR-diagram type plot. It is clear that the stars in the sample for Sculptor are more located in a more restricted area of the HR diagram than the halo stars. It was mentioned before that for the Sculptor spectroscopy only

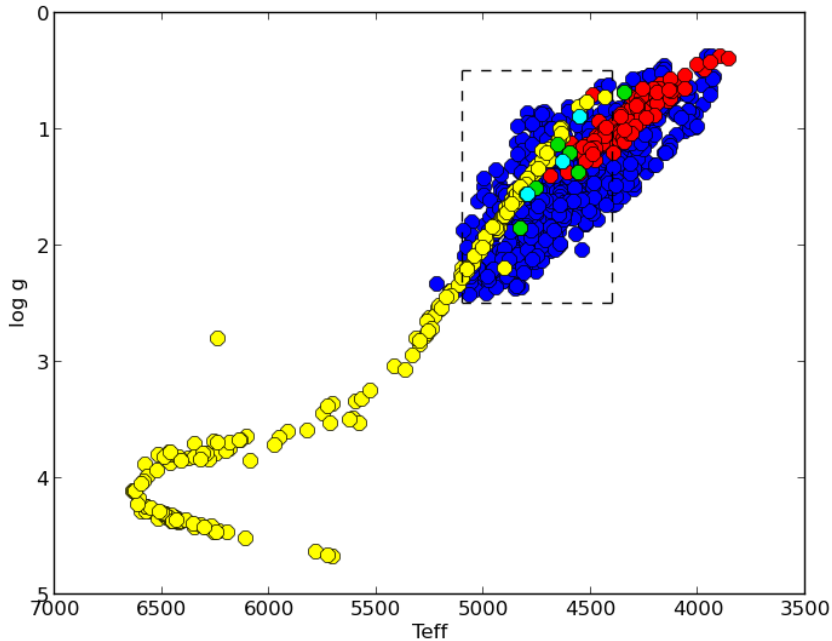


Figure 3.3 *HR diagram of all stars in the halo and Sculptor. Yellow circles are halo stars, blue circles are stars from the LR Sculptor sample, red circles are stars from the HR Sculptor sample (notice that these are located at the tip of the RGB), cyan circles are the three stars from Frebel et al. (2010) and Tafelmeyer et al. (2010) and green circles are stars from Starkenburg et al. (2010). The region indicated with dashed lines is the region where halo giant stars are found.*

stars were chosen that were quite high up the RGB because they are the brightest and give the best signal to noise. For the halo, the sample covers a larger part of the HR diagram. It shows some stars on the main sequence and the main sequence turnoff is clearly visible. When comparing stars we need to be sure that they are similar types of stars. We will only use the giant stars from the halo Yong et al. sample, because all the Sculptor stars in our sample are giants. After inspecting the HR diagram, we chose the limit in  $\log g$  to be where the Sculptor sample stops. We will use the term giant for stars with  $\log g \leq 2.5$ . See the dashed lines in Figure 3.3 for the region of the halo giant stars.

One of the reasons why we wanted to make this kind of plot was to see whether the Sculptor RGB was in a different area on the HR diagram than the halo RGB. We started with only the HR Sculptor sample (the red circles in Figure 3.3) plus the extra 10 HR/MR stars that we added (green and cyan circles in Figure 3.3). It looked like the Sculptor RGB had a slightly different slope and was located  $\sim 200\text{K}$  towards lower temperatures than the halo RGB. We wanted to know what the RGB of Sculptor looked like for higher  $\log g$  (so lower on the RGB) to see if the apparent slope would continue and if maybe the two samples would get closer to each other at some point. So we extended our Sculptor sample by analyzing a larger LR sample (blue circles in Figure 3.3). This increased our range in Sculptor in  $\log g$  quite a bit. There is now a larger range over which we can compare the two samples, and there is no obvious offset anymore.

What can be seen from Figure 3.3 is that the scatter in the Sculptor samples is a lot bigger than the scatter in the halo Yong et al. sample. The LR sample has the most scatter, but that is because for the LR sample the spectroscopy is as the name says, low resolution. The metallicity is estimated from this spectroscopy, and the derivation of  $T_{eff}$  depends partially on the metallicity, as well as the bolometric correction used in deriving  $\log g$ . The LR  $[\text{Fe}/\text{H}]$  estimate gives rise to more scatter. We wanted to find out why the halo has so little scatter compared to the HR Sculptor sample, and we came to a conclusion that it is because the values for  $\log g$  are determined in different ways for the two systems. For the halo, the  $\log g$  values are determined using isochrones, which are theoretical lines on the HR diagram for stars of a

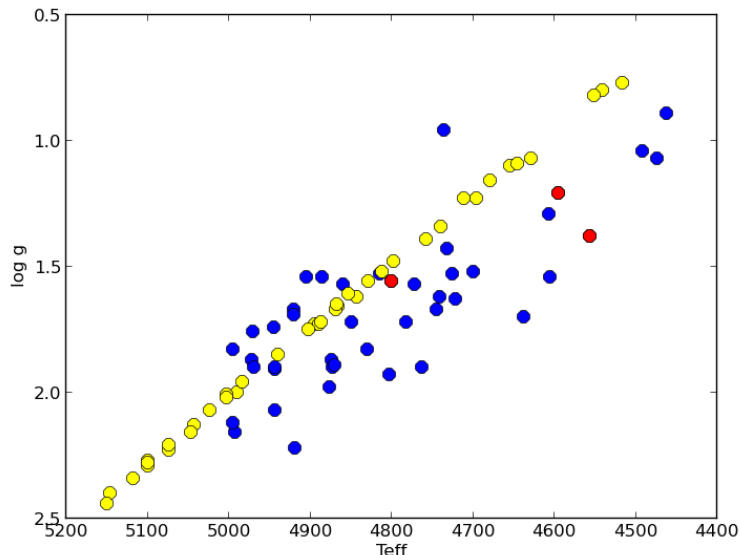


Figure 3.4 HR diagram for stars in the range  $-3.0 \leq [\text{Fe}/\text{H}] \leq -2.5$ . LR Sculptor sample is shown in blue, HR/MR Sculptor sample is shown in red and halo stars are shown in yellow

constant age. All the halo stars are pushed artificially onto this isochrone, which makes it look so narrow and unscattered. They have to assume an isochrone because the halo stars are all at different distances which makes it hard to derive  $\log g$  photometrically. For the Sculptor stars we did not make use of isochrones but determined  $\log g$  in a different way, as described in Section 2.2. We do not use theoretical isochrones and get a larger scatter.

### 3.2.1 Metallicity dependence

It is not strange that the samples do not fall exactly on top of each other. Isochrones are among other things dependent on metallicity. The average metallicity of our Sculptor sample is higher than that of the Yong et al. halo sample as is shown in Figure 3.1. When we look at the giant stars but with only a certain metallicity range for both samples, we can compare the locations on the HR diagram of similar metallicity stars. If we choose this range to be  $-3.0 \leq [\text{Fe}/\text{H}] \leq -2.5$  and plot again, Figure 3.4 is what we get. We choose this range because it is quite narrow and it covers the lowest metallicity part of the range where the halo and Sculptor samples have overlapping metallicities. There are 43 Sculptor stars in this range. What is noticeable is that there are only metal-poor stars in this range with temperatures higher than 4400K, while in Figure 3.3 it is clear that the Sculptor sample extends to lower temperatures. Where in the previous plot the RGBs were on average  $\sim 200\text{K}$  apart, they are only  $\sim 100\text{K}$  apart on average here. They are more in the same region as the halo stars than before. This is what we expected, since the halo stars are all quite metal-poor compared to the whole Sculptor sample, but now we are looking at the same metallicities.

Summarizing this chapter, we conclude that the Yong et al. halo sample and the Sculptor sample can be compared to each other, but with some caution.

# Chapter 4

## CEMP stars

In this study we are specifically interested in Carbon Enhanced Metal-Poor (CEMP) stars. Many of these stars have been found in the halo, but very little to none in most dSph systems. In Sculptor, only one CEMP star has been confirmed to this day (Skúladóttir et al. in prep.) This is interesting because we think that the halo and dSph systems should look similar, or at least their old populations should. Then why is it that we do not find more CEMP stars in Sculptor? Are we looking in the wrong place? Are they not there? Do we just not recognise them? To try to answer this question about the number of CEMP stars in Sculptor, we will first look at the CEMP stars in the Yong et al. halo sample and look at their distributions in metallicity, effective temperature and surface gravity.

### 4.1 CEMP stars in the halo

For the Yong et al. halo sample, carbon to iron ratios are given for 176 stars. See Figure 4.1, where  $[C/Fe]$  is plotted against luminosity. In this figure the Aoki et al. CEMP definition limit has been plotted, and CEMP stars have been indicated by red circles. There are also stars in this sample that have only upper limits for carbon. They are not regarded as CEMP stars in

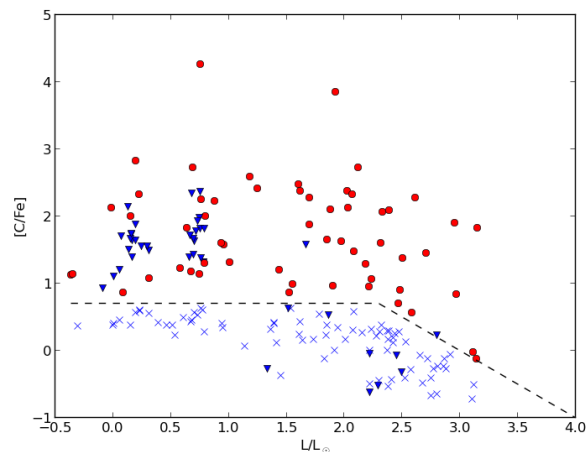


Figure 4.1 *Plotted is the carbon abundance as a function of luminosity for the Yong et al. halo sample. Red dots are CEMP stars, blue crosses are normal stars and blue triangles indicate stars for which only a carbon upper limit is available. Also plotted is the CEMP criterium limit from Aoki et al. (2007) as a black dashed line.*

the rest of this study (even though they might be above the limit) because we do not have a good value for  $[C/Fe]$ . These stars and the stars for which we do not have carbon abundances at all are treated as non-CEMP stars. There are 57 CEMP stars in this sample, which include all the subclasses of CEMP stars. The majority of the CEMP stars in the Yong et al. halo sample can be classified as CEMP-no stars (Yong et al. 2013b). In Figure 4.2 we plot the HR diagram for the halo, but now with CEMP stars indicated in orange and normal stars in yellow. There is no obvious variation in CEMP fraction over the RGB. The total CEMP fraction in the Yong et al. halo sample is 23%.

Beers & Christlieb (2005) state that the number of CEMP stars increases with decreasing metallicity  $[Fe/H]$ . Lee et al. (2013) have confirmed this trend. Following Yong et al. (2013b), we plot the CEMP fraction for metallicities below  $[Fe/H] = -3.0$  in three bins with roughly equal amounts of stars, and one bin for  $[Fe/H] \leq -4.5$  with just three stars. See Figure 4.3. There is a very clear trend, but according to Yong et al. (2013b) this is not statistically significant. They concluded that nothing can be said about this apparent trend from this data set. When taking into account higher metallicities which are in their literature sample as well (but they did not use because they were only interested in the lowest metallicities), the trend becomes even less clear. In Figure 4.4 we show the CEMP fraction up to  $[Fe/H] = -2.0$ , using bins with roughly equal amounts of stars except for the lowest metallicity bin. When using only bins with roughly equal amounts of stars (so also for the lowest metallicity bin), Figure 4.5 is what we get. The strong trend one might deduce from Figure 4.3 is nowhere to be seen.

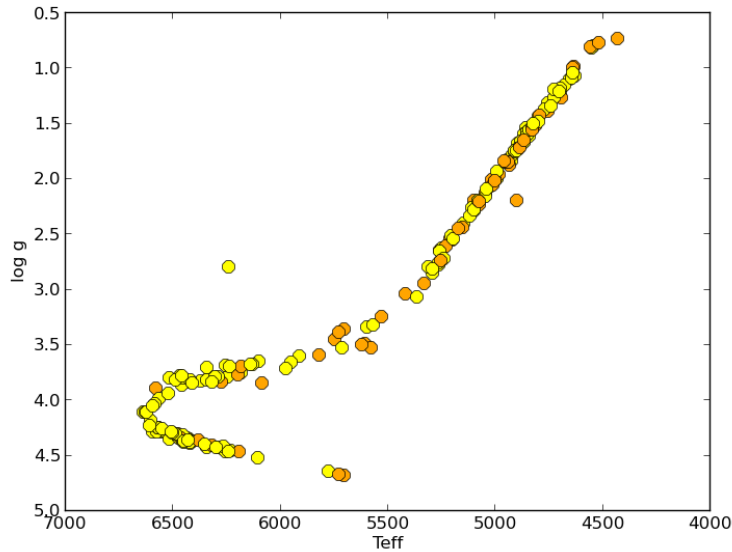


Figure 4.2 *CEMP stars in the halo. Normal halo stars are shown in yellow, CEMP stars in orange.*

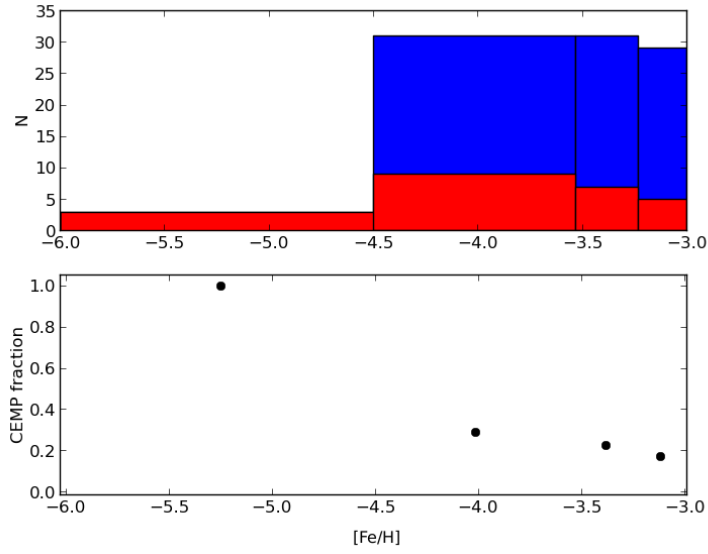


Figure 4.3 Upper panel: Bins for  $[Fe/H] \leq -3.0$  used to calculate halo CEMP fraction. Blue are the total number of stars in a certain range, red are the CEMP stars. Lower panel: CEMP fraction as a function of metallicity  $[Fe/H]$

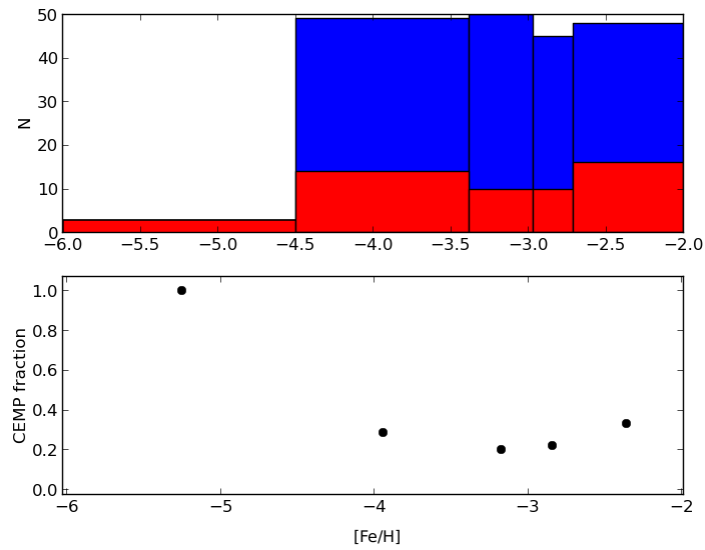


Figure 4.4 Same as in the previous figure, now for  $[Fe/H] \leq -2.0$

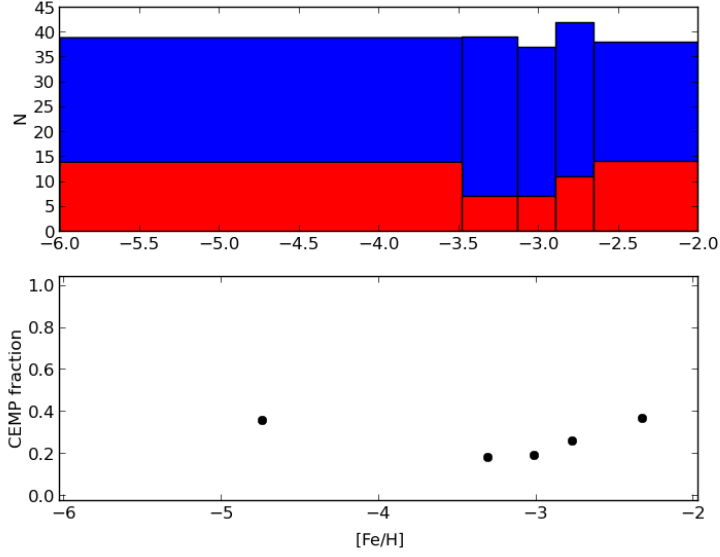


Figure 4.5 Same as in the previous figure, for  $[Fe/H] \leq -2.0$  and with roughly equal numbers in every bin

We are also interested in the distribution of CEMP stars in the halo in  $T_{eff}$  and  $\log g$ . If there are specific regions of the HR diagram that show more CEMP stars, then maybe this is also the case for a bias in comparing Sculptor to the halo. We made plots similar to the ones we show before but now for  $T_{eff}$  and  $\log g$ . We did the calculation for a specific range in  $T_{eff}$  and  $\log g$  only, because this is the range where the halo giants are. These ranges are  $4400 \leq T_{eff} \leq 5100$  and  $0.5 \leq \log g \leq 2.5$ , see the dashed lines in Figure 3.3 for a visualisation of this region. Figures 4.6 and 4.7 are the resulting figures for the CEMP fractions. There are no significant trends visible in the CEMP fractions, except that there does seem to be a peak around 5100K in Figure 4.6 and around 2.5 in Figure 4.7. If we choose equal width bins instead of bins with equal numbers of stars, the picture does not change. There might be a preferred position on the HR diagram for CEMP stars, on the lower part of the RGB. But this is not significant enough with the statistics this data set offers, and in the Sculptor sample there are not many stars in this region of the HR diagram. From this we conclude that it is not useful to assume a preferred location on the HR diagram for CEMP stars, and we assume that the halo CEMP fractions can be directly compared to those in Sculptor.

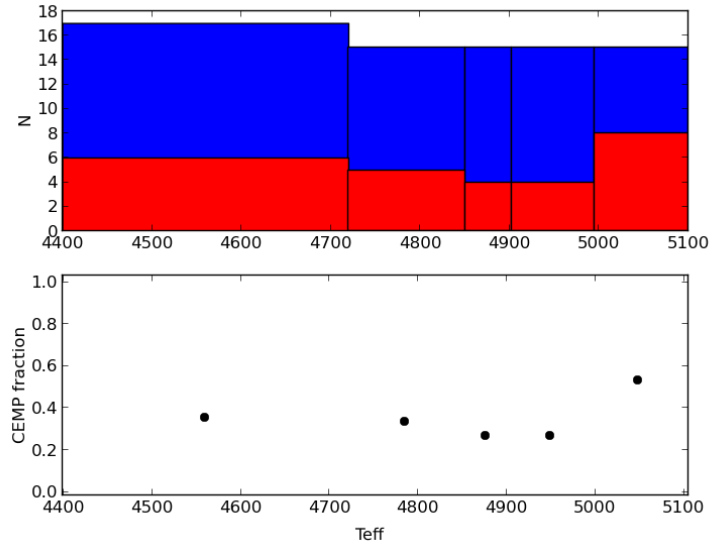


Figure 4.6 Same as in the previous figure, now for  $T_{eff}$  in the range  $4400 \leq T_{eff} \leq 5100$

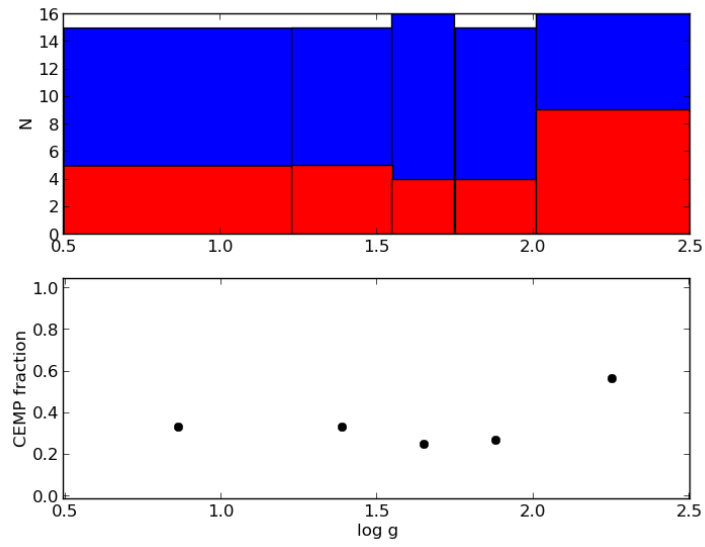


Figure 4.7 Same as in the previous figure, now for  $\log g$  in the range  $0.5 \leq \log g \leq 2.5$

## 4.2 CEMP stars in Sculptor

Only for a small number of stars in Sculptor carbon has been measured directly, and only one of these stars has a high  $[C/Fe]$  value and fits the CEMP criterium (Skúladóttir et al. in prep.). We will discuss here what this limits on CEMP stars in Sculptor compared to the halo.

### 4.2.1 Ása's star

There is one CEMP star in Sculptor, and it has been found by chance. For the stars of the HR Sculptor sample high resolution spectra were taken in the wavelength range  $\sim 9100-9300 \text{ \AA}$  as well to measure sulphur abundances in Sculptor. In these spectra CN lines are observable for stars down to  $[Fe/H] \sim -2.2$ , and there was one star (ET0097) which had unusually strong CN lines. The star has been followed up with high resolution spectroscopy over a large wavelength range (Skúladóttir et al. in prep.), and an accurate carbon abundance has been derived. It turned out to be a CEMP-no star.

We will call this star Ása's star because it has been found by Ása Skúladóttir (a PhD student working at the Kapteyn Institute). Ása's star has metallicity  $[Fe/H] = -2.03$ . In Hill et al. (in prep.), ET0097 has metallicity  $[Fe/H] = -1.91$ , but the more detailed spectroscopy has shown that the metallicity is somewhat lower. Ása's star has  $T_{eff} = 4383K$  and  $\log g = 0.8$ , which means that it is located at the tip of the RGB. See the yellow star in Figure 4.8. It has  $[C/Fe] = +0.51$ , which is the highest carbon to iron ratio measured to date in Sculptor. It is an evolved giant, and before mixing started playing a role in this star it probably had  $[C/Fe] \geq +0.8$ . The star is classified as a CEMP-no star, since it does not have overabundances in s- or r-process elements that are related to CEMP-r, -r/s or -s stars.

### 4.2.2 More CEMP candidates

After this single star had been found, people started looking for more of these spectra which might possibly show a signal that could be linked to the star being a CEMP star. But they did not find any more stars in the HR sample that show CEMP signatures. For the LR sample only the CaT region could be looked at. This type of spectroscopy is mainly meant for deriving a simple estimate of the metallicity from the strong CaT lines, but if there is a lot of carbon in a star it could also be detectable in the signal in the CaT spectroscopy region. These spectra could also be interpreted as just noisy, which was done before the search for CEMP stars started. The LR sample has been scanned for spectra which may show this extra noisy signature, and 9 candidates were selected. In the LR spectra the carbon lines might be flattened out and not visible at all, so it is difficult to say with certainty that the noise in the spectra is indeed created because there is lots of carbon in the star. The parts of the spectrum where carbon might be noticed are at the edges, which makes it even harder to fit synthetic spectra which could tell about the amount of carbon. To find out whether these candidate stars really are CEMP stars, follow up HR spectroscopy should be done.

See Table 4.2 in the Appendix for all the candidate CEMP stars and some of their properties. We plotted the CEMP candidates in Figure 4.8. Of the 9 CEMP candidate stars that were found, two stars have been indicated as carbon stars by Azzopardi et al. 1986. It is not certain that they actually are carbon stars, there is still a possibility that they are CEMP stars instead. All the candidates fall in the range of  $-2.92 \leq [Fe/H] \leq 1.40$ , but only two stars have  $[Fe/H] < -2.0$ . These happen to be the two Azzopardi stars. Most of the CEMP candidates have relatively high metallicities, which is worth noticing because in the halo it seems that at lower metallicity there are more CEMP stars.

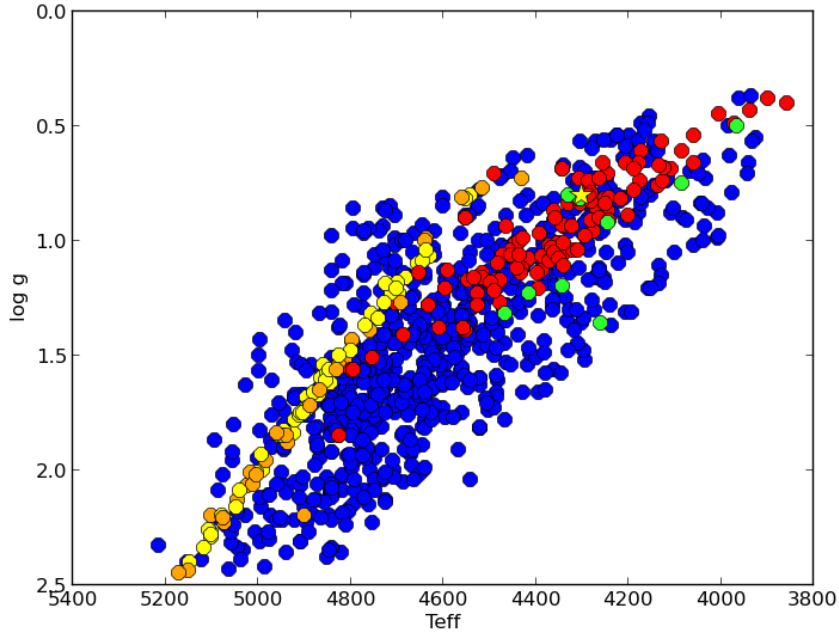


Figure 4.8 *HR diagram*, yellow circles = normal halo star, orange circles = halo CEMP star, blue circles = LR Sculptor star, red circles = HR Sculptor star. Yellow star is Ása's star, green circles are other CEMP candidates.

### 4.3 Some statistics

In the Sculptor samples, one CEMP star and 9 CEMP candidates are found. If we assume that the CEMP fractions in the halo and Sculptor are the same, we can use the binomial distribution of Equation 4.1 to calculate the probability of finding this number of CEMP stars or fewer in Sculptor,

$$\sum_{R=0}^C P(N, R, p) = \frac{N!}{R!(N-R)!} p^R (1-p)^{N-R} \quad (4.1)$$

where  $p$  is the underlying CEMP fraction assuming it is the same as the halo,  $N$  is the total number of stars observed in Sculptor and  $C$  is the number of CEMP stars. We will look at this probability in two different metallicity ranges.

**Metallicity range:**  $-2.0 \leq [\text{Fe}/\text{H}] \leq -1.0$

There is a known CEMP fraction in the stellar halo in this metallicity range, taken from Lee et al. 2013. In that paper, cumulative CEMP fractions are given for stars below a certain  $[\text{Fe}/\text{H}]$ . They also give the number of stars and CEMP stars, so from that we can calculate the CEMP fraction in this range. We find the CEMP fraction in the halo within the range of  $-2.0 \leq [\text{Fe}/\text{H}] \leq -1.0$  to be 5%. We have  $C = 7$  as the number of CEMP candidates in this metallicity range and  $N = 82 + 7 = 89$ . We take this number for  $N$  because it is the number of HR Sculptor stars that fall in this metallicity range plus the number of CEMP candidates which do not come from the HR sample. The probability of finding 7 CEMP stars or fewer in this case is 92%. If only 3 of the candidates actually are CEMP stars, the probability of this situation would be 34%.

We can also approach it from the other side, if we have a CEMP fraction and a number of stars in this range in Sculptor, how many CEMP stars would we expect to find? The expected number is  $R = Np \pm \sqrt{N(1-p)p}$ . In our case  $R = 4.5 \pm 2.1$ . The lowest amount of CEMP stars we could expect would then be 3.

**Metallicity range:**  $-3.0 \leq [\text{Fe}/\text{H}] \leq -2.0$

Now we use  $p = 0.19$  (calculated from the numbers of CEMP stars in this range from Lee et al. 2013),  $C = 3$  and  $N = 18 + 2 = 20$  for this metallicity range.  $N$  is again the number of HR Sculptor stars in this metallicity range plus the CEMP (candidate) stars that are not in the HR sample. The probability of finding 3 CEMP stars or fewer is 46%. The two CEMP candidate stars in this range are both indicated as carbon stars by Azzopardi et al. 1986. It is not very likely that these are actual CEMP stars. So we might also assume that there is just one CEMP star in this range, only Ása's star. The chance of finding just one CEMP star out of 20 is 8%.

Again we can calculate the number of CEMP stars we expect to find, taking the CEMP fraction and the number of stars in this metallicity range. The number we find is then  $R = 3.8 \pm 1.8$ . This means that we expect to find at least two CEMP stars in this range.

## 4.4 Conclusions

If all the CEMP candidate stars would be confirmed to be a CEMP star, the fraction of CEMP stars in the halo and in the HR Sculptor sample would be similar. But, if these are all the CEMP stars there are and not more will be found in the LR sample, there are far fewer CEMP stars in Sculptor than we would expect when assuming the same CEMP fraction as in the halo. It is also strange that the CEMP candidate stars that are found in Sculptor all have relatively high  $[\text{Fe}/\text{H}]$ . If the CEMP fraction increases with decreasing  $[\text{Fe}/\text{H}]$ , we would expect that if we find any CEMP stars in Sculptor at all, we would find them at lower  $[\text{Fe}/\text{H}]$ . But there are not so many stars that have very low  $[\text{Fe}/\text{H}]$  in Sculptor at all. Maybe there is a difference here between the halo and Sculptor distributions of CEMP stars.

# Summary and Discussion

In this work we have looked at metal-poor stars in the Milky Way halo and in Sculptor dSph. We do this because we want to know how similar or different these two systems are from each other. The standard assumptions that the halo has been build up by early mergers of dSph's, led us to ask the question why there are (almost) no CEMP stars in Sculptor but many in the halo. They should be in both systems if they are similar of origin. We studied our two samples for Sculptor and the halo by first looking thoroughly at the derivation of several physical parameters for the stellar populations. After that we plotted the samples on a  $T_{eff} - \log g$  HR diagram and looked at the differences and similarities there. We could not find any strong biases that could explain why there are less CEMP stars being found in Sculptor. The probability of finding the number of (candidate) CEMP stars in Sculptor that we have now is in quite good agreement with the CEMP fraction in the halo. But this is only the case if at least half of the CEMP candidates will be confirmed to actually be CEMP stars and if these are not the only CEMP stars present in Sculptor. It will be interesting to see HR spectroscopy of the CEMP candidates.

There are several limitations we had, assumptions we made and many more factors that we could have taken into account in this analysis. First of all we are limited in the amount of data that we have. We do not have good carbon abundances for most of the stars in Sculptor. We know that except for Ása's star, there are no more CEMP stars in the HR sample. For the LR sample, we are not sure because no full (HR) spectra are available. The CEMP candidates are all part of the LR sample. When calculating the CEMP fractions in Section 4.3 we are comparing the number of CEMP candidates from the LR sample with the non-CEMP stars from the HR sample. We do this because we are certain that there are no more CEMP stars in the HR sample, and for the LR sample we do not know this with certainty. But we are comparing stars from two different samples which may not be a perfectly correct thing to do.

It would also be interesting to have more (upper) RGB stars in the sample for the halo, to be able to compare stars of similar positions in their evolution on the HR diagram. Or more stars in Sculptor on the lower RGB, since this was also where we found that maybe there is a preferred location for CEMP stars in the halo. Now we only could do very small number statistics, which is not very reliable. But at least it does give an indication of what the situation with CEMP stars in Sculptor looks like.

We also assumed we could compare the derived effective temperatures for the halo and Sculptor, even though they have been derived in different manners. There could be an error in the derivation of temperature in one of the samples (or both), and it is more likely that this is the case for the Sculptor sample than for the halo. For the halo the derivation was very thoroughly done, and for Sculptor there were some uncertainties about differences between derived photometric temperatures which have not been explained yet. We also assumed we could compare the different values for  $\log g$  which also have been derived in different ways.

If we had more and better data, this could improve the existing idea we have of CEMP stars in general and specifically outside the Milky Way. But the perfect sample does not exist, and even if it did it would not be an easy task to make a careful comparison between the halo and Sculptor. It seems to be the case that for now, CEMP stars will remain something we do not really understand yet. Not in the halo, and not at all in other galaxies like Sculptor.

## Acknowledgements

I would like to thank Eline Tolstoy for her supervision for this bachelor project. She made me intrigued by the mystery of CEMP stars and motivated me to try and think of ways to address the issue. Also I would like to thank Ása Skúladóttir for answering some of my questions when I did not know how to continue and for sending me the draft paper on her CEMP star. I thank Eline Tolstoy, Ása Skúladóttir and Stefania Salvadori for their useful comments on this work in one of its final stages. I also would like to thank the Kapteyn Institute for providing a room, a desk and a computer to work on this project.

# References

- Alonso, A., Arribas, S., & Martínez-Roger, C. 1999, *A&A*, 140, 261
- Aoki, W., Beers, T. C., Christlieb, N., et al. 2007, *ApJ*, 655, 492
- Aoki, W., 2010, in *IAU Symp. 265, Chemical Abundances in the Universe: Connecting First Stars to Planets*, ed. K. Cunha, M. Spite, & B. Barbuy (Cambridge Univ. Press), 111
- Azzopardi, M., Lequeux, J. and Westerlund, B.E., 1986, *A&A*, 161, 232
- Battaglia, G., Helmi, A., Tolstoy, E., et al. 2008, *ApJ*, 681, L13
- Beers, T. C., Preston, G. W., & Shectman, S. A. 1985, *AJ*, 90, 2089
- Beers, T. C., Preston, G. W., & Shectman, S. A. 1992, *AJ*, 103, 1987
- Beers, T. C., & Christlieb, N. 2005, *ARA&A*, 43, 531
- de Boer, T. J. L., Tolstoy, E., Hill, V., et al. 2012, *A&A*, 539, A103
- Casagrande, L., Ramírez, I., Meléndez, et al., 2010, *A&A*, 512, A54
- Christlieb, N., Schörck, T., Frebel, A., et al. 2008, *A&A*, 484, 721
- Demarque, P., Woo, J., Kim, Y., & Yi, S. K. 2004, *ApJS*, 155, 667
- Frebel, A., Kirby, E. N., & Simon, J. D. 2010, *Nature*, 464, 72
- Helmi A., Irwin M.J., Tolstoy E., et al. 2006, *ApJ*, 651, L121
- Hill, V., Venn, K. A., Tolstoy, E., et al. (in preparation)
- Lucatello S., Tsangarides S., Beers T. C., et al. 2005, *ApJ* 625, 825
- Norris, J. E., Bessell, M. S., Yong, D., et al. 2013, *ApJ*, 762, 25
- Pietrzyński, G., Gieren, W., Szewczyk, O., et al. 2008, *AJ*, 135, 1993
- Ramírez, I. & Meléndez, J. 2005, *ApJ*, 626, 465
- Schlegel, D. J., Finkbeiner, D. P., & Davis, M. 1998, *ApJ*, 500, 525
- Skúladóttir, Á., Tolstoy, E., Salvadori, S., et al. (in preparation)
- Starkenburg, E., Hill, V., Tolstoy, E., et al. 2010, *A&A*, 513, A34
- Starkenburg, E., Hill, V., Tolstoy, E., et al. 2013, *A&A*, 549, A88
- Tafelmeyer, M., Jablonka, P., Hill, V., et al. 2010, *A&A*, 524, A58
- Tolstoy, E., Venn, K. A., Shetrone, M., et al. 2003, *AJ*, 125, 707
- Tolstoy, E., Hill, V., Irwin, M., et al. 2006, *ESO Messenger*, 123, 33
- Tolstoy, E., Hill, V., & Tosi, M. 2009, *ARA&A*, 47, 371
- Venn, K. A., Irwin, M., Shetrone, M., et al. 2004, *ApJ*, 128, 1177
- Wyse, R. F. G. & Gilmore, G. 2005, *astro-ph/0510025*
- Yanny, B., Rockosi, C., Newberg, H. J., et al. 2009, *AJ*, 137, 4377
- Yong, D., Norris, J. E., & Bessell, M. S. 2013 (a), *ApJ*, 762, 26
- Yong, D., Norris, J. E., & Bessell, M. S. 2013 (b), *ApJ*, 762, 27

Image of Figure 1.1: couldn't retrieve original source. Found the image on [http://www.poyntsource.com/Richard/ngc\\_5694\\_escaping\\_globular.htm](http://www.poyntsource.com/Richard/ngc_5694_escaping_globular.htm) (retrieved on the 28th of June 2014) and adapted it to fit our purpose of explaining the structure of the Milky Way

# Appendix

Table 4.1. Sample of LR Sculptor stars from Tolstoy et al. (2006)

Name	I (mag)	V (mag)	$T_{eff}$ (K)	log g cgs units	[Fe/H]
scl_25_060	19.19	20.12	4803	2.17	-0.55
scl_25_010	17.18	18.32	4363	1.19	-1.36
scl_25_024	17.49	18.57	4478	1.36	-1.93
scl_25_012	16.83	17.86	4562	1.13	-0.89
scl_25_020	18.03	19.03	4624	1.64	-0.93
scl_25_021	17.83	18.84	4598	1.54	-1.52
scl_25_014	17.10	18.47	4059	1.02	-1.40
scl_25_019	17.37	18.24	4924	1.48	-1.19
scl_25_029	17.25	18.40	4345	1.21	-1.26
scl_25_041	18.72	19.66	4747	1.95	-1.77
scl_25_028	17.38	18.22	4997	1.50	-1.42
scl_25_015	16.52	17.74	4243	0.88	-1.36
scl029_25_	18.11	19.25	4359	1.56	-0.96
scl_25_031	17.60	18.49	4885	1.54	-2.94
scl004_25_	15.98	17.03	4522	0.78	-1.49
scl033_06_	18.60	19.65	4520	1.82	-1.47
scl017_25_	17.42	18.46	4540	1.36	-1.53
scl019_06_	17.59	18.62	4558	1.43	-1.24
scl047tor_	19.29	20.16	4919	2.22	-2.97
scl027-10_	18.22	19.21	4639	1.71	-1.56
scl024tor_	18.14	19.08	4748	1.72	-1.42
scl011_07_	17.04	17.94	4840	1.31	-1.59
scl015_04_	17.11	18.44	4100	1.05	-1.32
scl020_06_	17.68	18.64	4703	1.52	-1.58
scl_05_002	15.96	17.14	4302	0.68	-1.39
scl039tor_	18.92	19.91	4641	2.00	-1.22
scl_05_030	17.99	19.10	4417	1.54	-1.63
scl_05_034	18.11	19.18	4482	1.61	-1.23
scl014tor_	16.56	17.75	4294	0.92	-1.61
scl030-10_	17.72	18.80	4467	1.45	-1.51
scl_05_035	18.08	18.97	4897	1.76	-0.68
scl_04_072	18.90	19.86	4728	2.03	-0.57
scl025-17_	17.70	18.61	4817	1.57	-1.49
scl013_04_	16.62	18.08	3976	0.79	-1.48
scl042_20_	18.32	19.44	4394	1.66	-0.80
scl_04_108	19.23	20.02	5214	2.33	-0.44
scl022-12_	17.88	18.76	4900	1.67	-1.16
scl_04_008	16.23	17.27	4551	0.89	-1.92
scl008_06_	16.76	17.68	4808	1.19	-2.45
scl039tor_	18.33	19.23	4843	1.83	-1.43
scl027-13_	17.85	18.73	4907	1.67	-0.98
scl_05_109	19.17	20.06	4883	2.19	-0.98
scl029_02_	17.60	18.76	4331	1.35	-1.37
scl_05_032	17.93	18.83	4846	1.67	-1.24
scl_05_033	17.97	18.91	4747	1.65	-1.71
scl_05_072	18.49	19.47	4675	1.84	-0.71
scl_05_102	19.24	20.14	4845	2.20	-1.35
scl013-10_	17.25	18.26	4607	1.31	-1.97
scl_04_009	16.89	18.08	4285	1.04	-1.34
scl037tor_	19.05	19.87	5085	2.21	-0.84
scl025tor_	17.62	18.52	4839	1.54	-1.68
scl_05_073	18.97	19.87	4843	2.09	-1.45
scl044_05_	18.35	19.30	4737	1.81	-0.89
scl001-10_	15.73	16.96	4237	0.56	-1.56
scl035_09_	17.76	18.98	4237	1.37	-1.16
scl009tor_	16.24	17.41	4361	0.82	-2.34
scl_05_014	16.51	17.71	4277	0.89	-1.52
scl_04_012	17.15	18.28	4379	1.19	-1.33
scl006tor_	16.35	17.31	4704	0.99	-1.69

Table 4.1 (cont'd)

Name	I (mag)	V (mag)	$T_{eff}$ (K)	log g cgs units	[Fe/H]
scl_05_013	16.93	18.18	4205	1.02	-1.46
scl044-12_	18.69	19.55	4948	2.01	-1.29
scl041_05_	18.26	19.18	4798	1.78	-2.29
scl_04_022	16.72	17.93	4263	0.97	-1.55
scl037_05_	17.89	19.00	4411	1.49	-1.24
scl008_07_	16.68	17.64	4714	1.12	-2.19
scl_04_164	19.51	20.50	4703	2.27	0.14
scl063_20_	19.29	20.17	4895	2.23	-1.40
scl_04_154	19.17	20.13	4724	2.13	-0.67
scl_04_149	19.03	19.97	4750	2.08	-1.33
scl021_06_	17.27	18.23	4717	1.36	-2.31
scl_04_162	19.38	20.33	4751	2.23	-0.62
scl_05_025	16.84	17.83	4640	1.16	-1.64
scl_04_064	17.97	18.97	4628	1.61	-2.12
scl_05_055	17.86	18.77	4824	1.63	-2.41
scl003_06_	17.69	18.65	4707	1.53	-2.00
scl058_02_	19.51	20.11	6097	2.70	0.12
scl_04_144	19.45	20.29	5030	2.35	-0.81
scl011_20_	16.52	17.52	4621	1.03	-1.68
scl_04_006	16.10	17.28	4318	0.74	-1.82
scl012_05_	18.22	19.29	4484	1.66	-0.94
scl_04_026	17.05	18.12	4482	1.19	-1.28
scl028_07_	17.53	18.74	4273	1.30	-1.82
scl005_06_	19.04	19.94	4842	2.11	-2.35
scl006_06_	18.41	19.47	4501	1.74	-1.25
scl033tor_	18.25	19.09	4995	1.83	-2.68
scl_04_062	17.90	18.93	4559	1.56	-1.08
scl_04_056	17.48	18.47	4639	1.42	-1.34
scl008_06_	18.82	19.76	4757	2.00	-1.01
scl_05_142	19.28	20.12	5006	2.27	-1.25
scl_04_058	17.78	18.79	4606	1.52	-1.97
scl023-17_	17.52	18.39	4915	1.53	-1.50
scl_04_090	18.80	19.70	4851	2.03	-1.12
scl011-10_	16.69	17.83	4365	1.00	-1.44
scl007_02_	16.58	17.48	4841	1.13	-1.43
scl001-13_	15.72	16.93	4270	0.57	-1.68
scl_04_082	18.37	19.36	4639	1.78	-1.53
scl024tor_	17.45	18.41	4731	1.43	-2.77
scl_04_136	19.15	20.00	4971	2.20	-1.47
scl051_03_	18.78	19.81	4566	1.91	-2.00
scl_05_123	19.38	20.23	4995	2.31	-0.91
scl_04_158	19.44	20.26	5153	2.40	-0.11
scl010_06_	18.28	19.35	4483	1.68	-1.35
scl011_06_	15.94	16.86	4794	0.86	-1.84
scl034_11_	18.06	18.89	5052	1.80	-0.87
scl_04_134	19.15	19.97	5069	2.24	-1.11
scl012_06_	16.54	17.64	4435	0.97	-1.60
scl013_06_	16.29	17.65	4065	0.70	-1.27
scl_04_153	19.19	20.11	4794	2.15	-2.10
scl014_06_	17.68	18.72	4557	1.47	-2.21
scl002-13_	16.01	16.96	4728	0.86	-1.90
scl013-13_	16.25	17.63	4053	0.68	-1.47
scl_04_021	16.61	17.81	4297	0.94	-1.97
scl_05_129	19.42	20.25	5043	2.34	-1.07
scl_04_047	17.24	18.28	4551	1.29	-1.99
scl023_05_	16.20	17.25	4524	0.86	-1.65
scl004_11_	16.20	17.15	4728	0.94	-1.91
scl015_06_	16.61	17.88	4178	0.88	-1.42
scl_04_024	17.12	18.52	4006	0.99	-0.88

Table 4.1 (cont'd)

Name	I (mag)	V (mag)	$T_{eff}$ (K)	log g cgs units	[Fe/H]
scl027-10_	17.44	18.73	4156	1.21	-1.53
scl045-10_	18.31	19.44	4379	1.65	-1.37
scl015-06_	18.64	19.59	4732	1.91	-2.30
scl049-14_	18.88	19.74	4943	2.07	-2.71
scl_04_016	16.76	17.73	4681	1.15	-1.38
scl026-05_	17.77	18.71	4758	1.57	-2.35
scl017-06_	18.84	19.75	4817	2.03	-1.53
scl036tor_	18.56	19.64	4465	1.78	-1.45
scl018-06_	17.24	18.54	4132	1.11	-1.19
scl_05_125	19.05	19.94	4872	2.13	-1.27
scl_05_044	17.53	18.46	4772	1.48	-1.95
scl_04_063	17.94	18.96	4597	1.58	-2.35
scl_05_024	16.56	17.69	4383	0.95	-1.49
scl021-10_	17.36	18.52	4335	1.25	-1.52
scl005-04_	15.95	17.26	4142	0.61	-1.67
scl_04_048	17.41	18.42	4598	1.38	-1.23
scl020-06_	18.75	19.73	4670	1.93	-2.32
scl020-03_	17.57	18.52	4734	1.49	-0.97
scl_04_005	15.90	17.20	4183	0.62	-2.13
scl042-08_	18.31	19.22	4840	1.83	-0.78
scl022-06_	18.90	19.85	4726	2.02	-1.98
scl_04_061	17.80	18.82	4593	1.53	-2.21
scl_05_026	17.01	17.99	4662	1.24	-1.77
scl024-06_	17.31	18.63	4128	1.15	-1.69
scl_05_042	17.42	18.34	4793	1.45	-1.80
scl039-05_	17.57	18.58	4607	1.44	-2.02
scl_04_057	17.53	18.59	4511	1.39	-1.88
scl_04_029	16.80	18.22	4006	0.88	-1.35
scl029-06_	19.02	19.99	4684	2.05	-1.26
scl036-10_	18.00	18.99	4640	1.63	-1.64
scl006-10_	16.28	17.50	4243	0.78	-1.37
scl_04_077	18.25	19.15	4839	1.79	-1.86
scl_04_081	18.42	19.34	4799	1.85	-2.38
scl_04_152	19.18	20.12	4760	2.15	-0.94
scl031-06_	17.04	17.97	4773	1.29	-2.00
scl046tor_	18.60	19.65	4520	1.82	-1.34
scl032-06_	17.15	18.26	4434	1.21	-2.07
scl_04_086	18.92	19.77	4978	2.11	-1.24
scl003-06_	15.99	16.95	4713	0.85	-2.11
scl033tor_	16.90	17.85	4735	1.22	-2.22
scl013-05_	18.08	18.98	4849	1.72	-2.52
scl_04_031	17.07	18.46	4038	1.00	-1.40
scl049-05_	16.95	18.04	4467	1.14	-2.05
scl036-06_	15.89	17.34	3982	0.50	-1.43
scl_04_020	16.81	17.84	4561	1.12	-1.62
scl_04_084	18.90	19.77	4939	2.10	-0.90
scl_04_085	18.93	19.88	4730	2.04	-1.17
scl_04_140	19.45	20.34	4906	2.31	-0.57
scl038tor_	18.19	19.17	4661	1.71	-1.26
scl039tor_	16.88	17.97	4484	1.12	-2.41
scl_04_019	16.74	17.90	4365	1.02	-2.20
scl040-06_	16.52	17.74	4284	0.90	-2.22
scl010-10_	16.50	17.78	4172	0.84	-1.57
scl_04_050	17.82	18.84	4605	1.54	-2.55
scl_04_091	18.87	19.85	4666	1.98	-2.14
scl019-12_	17.85	18.76	4825	1.64	-1.13
scl042tor_	18.17	19.13	4707	1.72	-2.05
scl_04_055	17.45	18.42	4684	1.42	-1.88
scl_04_059	18.07	19.00	4769	1.70	-1.68

Table 4.1 (cont'd)

Name	I (mag)	V (mag)	$T_{eff}$ (K)	log g cgs units	[Fe/H]
scl044tor_	16.55	17.78	4254	0.90	-1.92
scl059tor_	17.62	18.63	4605	1.46	-1.93
scl045tor_	18.51	19.48	4689	1.85	-0.98
scl_04_027	17.18	18.30	4410	1.21	-1.88
scl019_05_	16.88	17.90	4581	1.16	-1.68
scl020_05_	17.63	18.55	4814	1.53	-2.79
scl022_20_	17.84	18.76	4793	1.62	-1.51
scl_04_018	16.68	17.78	4454	1.03	-2.12
scl066tor_	18.93	19.87	4747	2.04	-1.68
scl_04_060	18.15	19.11	4703	1.71	-1.66
scl_04_089	18.44	19.33	4874	1.87	-2.75
scl026_25_	18.07	18.99	4796	1.71	-2.17
scl012_11_	17.09	18.33	4221	1.10	-1.53
scl069_05_	15.79	17.00	4277	0.60	-1.84
scl049tor_	16.77	17.76	4639	1.14	-1.49
scl_04_023	17.18	18.18	4618	1.29	-1.41
scl004-10_	16.34	17.32	4661	0.97	-1.60
scl014-13_	16.56	17.69	4384	0.95	-1.56
scl030-20_	18.17	19.32	4344	1.58	-1.22
scl021tor_	17.58	18.51	4772	1.50	-1.98
scl028_05_	18.17	19.10	4772	1.74	-2.06
scl053tor_	16.76	17.90	4379	1.03	-1.87
scl029_11_	17.80	18.72	4796	1.60	-1.34
scl056tor_	18.30	19.23	4774	1.79	-2.18
scl030_11_	17.92	18.82	4839	1.66	-1.74
scl057tor_	18.07	19.00	4775	1.71	-1.20
scl074tor_	16.40	17.65	4208	0.81	-1.53
scl061tor_	18.68	19.65	4683	1.91	-1.90
scl062_03_	18.67	19.66	4644	1.89	-2.00
scl065tor_	18.09	19.09	4624	1.65	-1.96
scl077tor_	18.26	19.17	4819	1.79	-2.17
scl078tor_	18.34	19.28	4756	1.8	-2.36
scl032_11_	17.23	18.19	4704	1.34	-1.73
scl067tor_	17.02	18.10	4483	1.18	-2.06
scl068tor_	18.28	19.29	4601	1.73	-1.05
scl069tor_	17.5	18.54	4545	1.39	-1.78
scl070tor_	18.24	19.22	4660	1.73	-1.46
scl072_03_	17.00	18.09	4466	1.16	-2.04
scl019_20_	17.41	18.39	4662	1.40	-1.74
scl081tor_	18.00	18.98	4661	1.63	-1.76
scl008-15_	16.44	17.73	4151	0.80	-1.38
scl082tor_	19.03	19.96	4771	2.09	-1.52
scl013_06_	17.19	18.39	4272	1.16	-1.41
scl074_03_	16.84	17.96	4414	1.08	-1.95
scl075_03_	17.63	18.63	4620	1.47	-1.64
scl076tor_	17.13	18.22	4453	1.21	-1.66
SCL2008	16.63	17.90	4193	0.90	-1.75
scl077tor_	16.57	17.80	4250	0.91	-1.86
scl086_02_	18.17	19.08	4824	1.75	-2.46
scl079tor_	18.37	19.22	4971	1.87	-2.79
scl081tor_	17.55	18.55	4620	1.44	-1.66
scl091tor_	17.79	18.74	4731	1.57	-2.11
scl084tor_	17.30	18.40	4438	1.27	-1.74
scl085_03_	18.46	19.45	4645	1.81	-2.06
scl034_11_	18.38	19.41	4559	1.75	-1.15
scl087tor_	17.52	18.42	4841	1.51	-1.51
scl094tor_	17.21	18.32	4428	1.23	-1.93
scl095tor_	17.14	18.19	4542	1.25	-2.23
scl089_03_	18.91	19.81	4839	2.06	-1.96

Table 4.1 (cont'd)

Name	I (mag)	V (mag)	$T_{eff}$ (K)	log g cgs units	[Fe/H]
scl099tor_	17.34	18.43	4468	1.30	-2.11
scl090tor_	18.00	18.98	4661	1.63	-1.73
scl103tor_	18.89	19.85	4706	2.00	-2.06
scl036_02_	18.93	19.93	4651	2.02	-0.27
scl092tor_	18.5	19.43	4771	1.87	-2.01
scl017_14_	16.74	18.14	4027	0.86	-1.38
scl011_09_	17.31	18.28	4701	1.37	-2.46
scl_02_115	18.19	19.09	4842	1.77	-2.14
scl093tor_	17.85	18.78	4779	1.61	-2.33
scl095tor_	18.93	19.88	4726	2.03	-1.90
scl114tor_	17.67	18.91	4205	1.31	-0.97
scl_03_207	18.41	19.43	4594	1.77	-2.32
scl100tor_	17.76	18.75	4641	1.53	-1.75
scl101tor_	17.40	18.50	4433	1.31	-1.56
scl116tor_	17.61	18.65	4545	1.43	-1.79
scl103tor_	18.38	19.33	4731	1.81	-2.19
scl_02_117	17.42	18.42	4626	1.39	-1.96
scl118tor_	17.93	18.91	4669	1.60	-2.17
scl106tor_	17.58	18.57	4643	1.46	-1.85
scl119tor_	16.64	17.75	4437	1.01	-2.10
scl040_02_	16.37	17.66	4156	0.78	-1.48
scl121tor_	18.41	19.34	4776	1.83	-2.32
scl108_03_	17.58	18.46	4904	1.54	-2.78
scl_03_043	17.03	18.09	4525	1.20	-2.24
scl125tor_	17.29	18.37	4471	1.28	-1.68
scl126tor_	17.25	18.23	4660	1.33	-1.60
scl127tor_	16.93	18.00	4486	1.14	-1.55
scl012tor_	16.66	17.62	4703	1.11	-1.68
scl128tor_	18.30	19.24	4748	1.78	-1.90
scl117tor_	19.02	19.92	4843	2.11	-1.47
scl130tor_	18.47	19.33	4943	1.91	-2.62
scl131tor_	17.77	18.77	4626	1.53	-2.02
scl132tor_	17.01	17.93	4792	1.28	-1.62
scl137tor_	18.56	19.46	4840	1.92	-2.09
scl119tor_	17.67	18.50	5025	1.63	-1.39
scl141tor_	17.31	18.34	4583	1.33	-2.37
scl143tor_	18.08	19.26	4294	1.52	-0.70
scl_02_386	19.55	20.39	5036	2.39	-0.72
scl020_03_	17.54	18.76	4239	1.28	-1.23
scl_14_021	16.23	17.16	4771	0.97	-1.40
scl036_11_	19.20	20.15	4725	2.14	-1.50
scl045_02_	16.15	17.38	4246	0.73	-1.75
scl145tor_	18.07	19.02	4726	1.68	-1.87
SCL2007	16.69	17.65	4703	1.13	-1.56
scl147tor_	17.56	18.58	4582	1.43	-1.76
scl148tor_	17.62	18.67	4520	1.43	-1.42
SCL2057	19.43	20.32	4908	2.31	-0.54
scl046_11_	18.27	19.33	4508	1.69	-0.65
scl016_08_	17.23	18.44	4251	1.16	-1.11
scl_14_023	16.91	17.93	4595	1.17	-2.18
scl_02_096	18.05	18.91	4944	1.74	-2.57
scl134tor_	17.95	18.91	4721	1.63	-2.57
scl_02_040	16.63	17.72	4474	1.02	-2.18
scl031_07_	18.57	19.62	4520	1.81	-1.17
scl157tor_	18.37	19.30	4772	1.82	-2.05
scl_02_107	17.99	18.88	4880	1.71	-1.01
scl_14_060	18.22	19.09	4939	1.83	-0.89
scl_02_382	19.34	20.18	5058	2.32	-0.44
scl033_06_	18.88	19.77	4870	2.06	-1.33

Table 4.1 (cont'd)

Name	I (mag)	V (mag)	$T_{eff}$ (K)	log g cgs units	[Fe/H]
scl_11_035	18.14	19.27	4378	1.58	-0.66
scl007_11_	16.60	17.59	4640	1.07	-1.63
scl159tor_	18.54	19.47	4770	1.89	-1.93
scl161tor_	17.79	18.79	4624	1.54	-1.91
scl_03_114	17.40	18.45	4542	1.35	-2.26
scl_02_043	16.62	17.61	4639	1.08	-1.48
scl_11_055	18.47	19.29	5055	1.96	-1.38
scl_02_104	17.57	18.58	4598	1.44	-1.38
scl_11_034	17.78	18.91	4381	1.44	-1.45
scl_14_041	18.05	18.95	4846	1.72	-1.26
scl147_03_	18.70	19.68	4664	1.91	-2.01
scl_03_007	15.89	17.20	4142	0.59	-1.67
scl_14_045	17.87	18.80	4771	1.62	-1.96
scl_14_012	16.09	17.05	4704	0.89	-1.73
scl_03_033	16.80	17.82	4597	1.13	-2.2
scl_03_044	16.21	17.42	4315	0.80	-2.46
scl_02_067	17.14	18.18	4545	1.25	-1.75
scl_03_097	17.22	18.20	4676	1.32	-2.32
scl_03_003	15.92	17.18	4188	0.61	-1.33
scl059_02_	17.46	18.49	4568	1.38	-1.96
scl060_11_	17.26	18.25	4652	1.33	-2.19
scl_03_005	15.89	16.97	4470	0.72	-1.61
scl174tor_	17.85	18.75	4841	1.64	-1.53
scl175tor_	17.76	18.76	4629	1.52	-2.11
scl177tor_	17.48	18.43	4732	1.45	-2.13
scl061_02_	17.44	18.44	4623	1.40	-1.85
scl_03_204	18.24	19.20	4703	1.75	-1.67
scl062_02_	15.71	16.94	4251	0.56	-1.84
scl_02_322	19.24	20.06	5056	2.27	-1.41
scl_02_101	18.25	19.19	4750	1.77	-1.29
scl_02_072	17.25	18.29	4551	1.29	-2.00
scl_03_342	18.95	19.91	4705	2.03	-1.97
scl_02_029	16.75	17.88	4381	1.03	-1.41
scl_03_049	16.67	17.76	4462	1.03	-1.92
scl_02_121	17.88	18.76	4919	1.69	-0.76
scl_02_109	17.98	18.89	4816	1.68	-1.94
scl_03_035	17.12	18.08	4712	1.30	-2.14
scl_03_036	17.10	18.17	4485	1.21	-1.52
scl032_20_	17.83	18.82	4640	1.56	-1.22
scl_03_106	17.64	18.75	4437	1.41	-2.20
scl_11_003	15.71	16.80	4449	0.64	-1.43
scl192tor_	17.56	18.40	4997	1.57	-1.39
scl_03_040	16.55	17.53	4664	1.05	-1.86
scl_02_120	17.75	18.68	4775	1.57	-2.14
scl_03_110	17.28	18.31	4559	1.31	-1.48
scl_03_098	17.43	18.39	4707	1.42	-1.94
scl193tor_	17.61	18.53	4793	1.52	-1.90
scl_02_035	17.02	18.09	4491	1.18	-1.79
scl_03_199	18.38	19.28	4840	1.85	-1.66
SCL2044	18.72	19.64	4794	1.97	-1.54
scl_02_114	18.09	19.02	4771	1.71	-1.46
scl_03_002	16.00	17.01	4600	0.81	-1.59
scl_11_056	18.43	19.28	4969	1.90	-2.65
scl_03_115	17.42	18.42	4642	1.39	-2.49
scl_03_050	16.77	17.88	4439	1.06	-2.16
scl_02_086	17.76	18.72	4711	1.55	-2.16
scl_03_107	17.95	18.90	4725	1.64	-1.65
scl_11_038	17.92	18.91	4640	1.60	-1.23
scl_02_073	17.36	18.35	4649	1.37	-2.11

Table 4.1 (cont'd)

Name	I (mag)	V (mag)	$T_{eff}$ (K)	log g cgs units	[Fe/H]
scl025_06_	18.38	19.20	5055	1.92	-1.37
SCL2006	16.70	17.63	4770	1.15	-1.47
SCL2031	17.93	19.05	4399	1.51	-1.56
scl_02_122	17.98	18.88	4839	1.69	-1.70
scl_14_017	16.54	17.49	4725	1.08	-1.39
scl_11_012	16.31	17.42	4462	0.89	-2.53
scl_02_071	17.18	18.20	4597	1.28	-2.24
scl_02_075	17.29	18.37	4464	1.28	-1.13
scl_11_054	18.29	19.23	4747	1.78	-1.69
scl_03_102	17.24	18.15	4824	1.38	-2.32
scl_03_121	17.63	18.63	4625	1.47	-1.96
scl015-17_	17.42	18.40	4661	1.40	-1.72
scl071_11_	17.44	18.64	4278	1.26	-1.58
scl_03_053	16.95	18.02	4489	1.15	-1.68
scl_03_052	16.81	18.00	4287	1.01	-1.38
scl_03_119	17.46	18.54	4468	1.35	-1.56
scl_03_117	17.57	18.57	4631	1.45	-2.19
scl_02_034	16.99	18.06	4486	1.16	-1.54
scl_14_014	16.68	18.01	4106	0.88	-1.43
scl_03_030	16.78	17.76	4677	1.15	-2.29
SCL2005	16.99	18.05	4506	1.17	-1.66
scl077_02_	15.70	16.94	4222	0.54	-1.51
scl_03_006	15.84	17.15	4142	0.57	-1.66
scl_02_069	17.15	18.16	4603	1.27	-1.79
scl_02_111	18.02	18.92	4848	1.70	-2.47
scl_02_030	16.71	17.89	4298	0.97	-1.21
scl_02_032	17.00	18.04	4568	1.20	-2.42
scl_14_024	17.14	18.12	4673	1.29	-2.21
scl_02_116	17.29	18.37	4464	1.28	-1.22
scl_02_112	18.04	18.95	4816	1.70	-1.80
scl080_11_	18.27	19.21	4749	1.77	-1.94
scl_03_048	16.54	17.77	4233	0.88	-1.46
scl_02_074	17.42	18.40	4660	1.40	-1.57
scl_03_051	16.84	17.96	4404	1.07	-1.70
scl_03_113	17.42	18.39	4688	1.41	-2.04
scl_02_028	16.65	17.75	4444	1.01	-1.88
scl_03_215	18.31	19.24	4772	1.80	-2.07
scl081_02_	16.62	17.88	4205	0.91	-1.74
scl_02_148	17.97	18.94	4681	1.63	-1.58
scl_03_145	17.57	18.64	4482	1.40	-1.20
scl_03_057	16.66	17.70	4541	1.05	-1.55
scl_03_174	17.99	18.91	4802	1.67	-2.42
scl_03_169	17.61	18.58	4682	1.49	-1.66
scl083_11_	19.06	19.90	4992	2.16	-2.67
scl_03_078	17.09	18.12	4563	1.23	-1.73
scl_02_161	17.45	18.45	4619	1.40	-1.56
scl_02_063	17.01	17.98	4691	1.25	-2.12
scl_03_178	18.08	19.01	4776	1.70	-2.27
scl_11_069	18.80	19.66	4960	2.06	-1.01
scl_03_058	16.51	17.68	4330	0.91	-1.77
scl_03_173	17.69	18.69	4624	1.49	-1.92
scl_03_065	16.95	18.08	4382	1.11	-1.50
scl_02_060	16.50	17.65	4353	0.92	-1.57
scl_02_141	17.49	18.44	4735	1.45	-2.26
scl_03_166	17.49	18.46	4689	1.44	-2.09
scl_02_065	16.95	17.98	4581	1.18	-2.27
scl_02_245	18.22	19.15	4778	1.77	-1.09
scl_02_156	17.19	18.25	4501	1.25	-1.34
scl_03_519	19.63	20.45	5062	2.43	-1.29

Table 4.1 (cont'd)

Name	I (mag)	V (mag)	$T_{eff}$ (K)	log g cgs units	[Fe/H]
scl_03_013	15.97	17.28	4136	0.61	-1.55
scl085_11_	18.98	19.82	4995	2.12	-2.92
scl_03_074	16.45	17.54	4487	0.95	-2.44
scl_02_145	17.73	18.65	4792	1.57	-1.66
scl047_20_	18.75	19.57	5084	2.09	-0.85
scl_03_237	18.26	19.18	4801	1.78	-2.42
scl046_25_	18.43	19.46	4578	1.77	-2.43
scl_02_134	17.89	18.76	4920	1.67	-2.52
scl_03_155	18.05	19.02	4688	1.66	-2.10
scl_03_132	17.25	18.30	4536	1.29	-2.08
scl043tor_	18.37	19.30	4769	1.82	-1.73
scl_02_166	17.77	18.73	4703	1.56	-1.68
scl_03_164	18.18	19.14	4704	1.72	-1.85
scl_14_028	16.75	17.80	4543	1.09	-2.23
scl_03_176	18.07	18.97	4844	1.72	-2.29
SCL2020	16.32	17.64	4117	0.74	-1.41
SCL2052	18.81	19.68	4920	2.05	-1.36
scl_02_159	17.39	18.34	4725	1.41	-1.63
scl_02_135	17.76	18.76	4618	1.52	-1.46
scl011_14_	17.93	19.01	4464	1.53	-1.28
scl_11_063	18.84	19.73	4906	2.07	-0.55
scl_03_235	18.25	19.15	4839	1.79	-1.88
scl_03_236	18.20	19.18	4660	1.71	-1.55
scl_03_153	18.00	18.99	4646	1.63	-2.04
scl_03_087	17.10	18.10	4621	1.26	-1.74
scl_02_256	18.16	19.02	4943	1.80	-1.44
scl_03_507	19.12	20.16	4541	2.04	-1.68
scl_03_172	17.49	18.65	4326	1.30	-1.01
scl_02_260	18.22	19.14	4792	1.77	-1.66
scl011_20_	16.42	17.38	4703	1.02	-1.51
scl_03_062	16.83	17.99	4332	1.04	-1.40
scl_14_031	16.48	17.62	4361	0.91	-1.24
SCL2016	17.06	18.20	4365	1.14	-1.43
scl_03_055	16.31	17.54	4246	0.80	-1.76
scl_03_471	19.36	20.25	4890	2.27	-0.83
scl_03_288	18.47	19.46	4639	1.82	-1.41
scl_02_138	17.19	18.34	4358	1.20	-1.74
scl015_03_	17.40	18.54	4362	1.28	-1.28
scl_02_445	19.09	19.97	4899	2.16	-1.22
scl_03_180	18.12	19.06	4748	1.72	-1.44
scl_11_040	17.69	18.59	4860	1.57	-2.87
scl_03_449	19.21	20.15	4803	2.18	-0.18
scl_03_161	18.04	19.05	4601	1.63	-1.74
scl_11_043	17.68	18.63	4727	1.53	-1.88
scl094_11_	17.75	18.78	4570	1.50	-2.07
scl149_15_	18.12	19.16	4547	1.64	-1.94
scl_11_065	18.22	19.14	4792	1.77	-1.75
scl095_02_	15.86	16.95	4452	0.70	-1.58
scl_11_008	15.92	17.20	4183	0.62	-1.77
scl_03_059	16.77	17.88	4474	1.07	-2.82
scl_03_242	18.21	19.20	4639	1.71	-1.54
scl_03_167	17.35	18.49	4362	1.26	-1.32
scl_02_160	17.33	18.34	4604	1.34	-1.87
scl_03_079	17.19	18.21	4607	1.29	-2.51
scl008tor_	16.10	17.11	4600	0.85	-1.60
scl_14_026	16.12	17.31	4308	0.75	-1.90
scl_03_083	16.76	17.86	4455	1.06	-2.15
scl018_03_	17.49	18.49	4640	1.42	-2.44
scl_14_048	17.04	17.93	4867	1.32	-1.39

Table 4.1 (cont'd)

Name	I (mag)	V (mag)	$T_{eff}$ (K)	log g cgs units	[Fe/H]
scl091-15_	17.53	18.51	4672	1.45	-2.21
scl_02_131	17.27	18.26	4640	1.34	-1.59
scl_02_155	18.13	19.09	4703	1.70	-1.52
scl_14_046	17.49	18.46	4693	1.44	-2.25
scl_03_075	16.64	17.58	4747	1.12	-1.46
scl_14_050	17.18	18.19	4601	1.29	-1.03
scl_02_151	17.96	18.93	4681	1.63	-1.45
scl022_03_	16.41	17.80	4031	0.73	-1.23
scl_02_444	19.29	20.20	4839	2.22	-0.82
SCL2015	16.61	17.61	4619	1.06	-1.49
scl_03_528	19.68	20.58	4850	2.38	-1.22
scl_03_063	16.95	18.04	4468	1.14	-2.10
scl023_03_	18.52	19.56	4583	1.83	0.07
scl_11_044	17.79	18.70	4816	1.60	-1.86
scl_02_146	17.68	18.71	4577	1.47	-2.27
scl_14_027	16.89	17.82	4770	1.23	-1.44
scl010tor_	17.03	18.07	4550	1.20	-1.93
scl025_03_	16.67	18.05	4042	0.84	-1.25
scl_02_456	19.45	20.28	5121	2.39	-0.11
scl026_03_	17.71	18.76	4520	1.47	-1.25
scl140tor_	18.13	19.11	4661	1.69	-1.76
scl_02_240	18.82	19.73	4817	2.02	-1.55
scl_11_062	18.24	19.13	4872	1.81	-1.22
scl_11_006	15.61	17.09	3960	0.38	-1.49
scl_11_005	15.68	16.87	4303	0.57	-1.79
scl025tor_	17.44	18.43	4650	1.40	-2.14
scl026tor_	19.01	19.92	4816	2.09	-1.71
scl027_03_	18.44	19.30	4943	1.90	-2.57
scl_14_032	16.68	18.06	4040	0.84	-1.21
scl_02_252	18.90	19.80	4840	2.06	-1.63
scl030tor_	18.60	19.49	4867	1.95	-1.44
scl038tor_	18.14	19.06	4793	1.74	-1.57
scl041_02_	16.60	17.80	4283	0.93	-1.69
scl_11_025	16.71	17.84	4383	1.01	-1.51
scl033tor_	17.73	18.67	4761	1.56	-2.46
scl024tor_	16.78	17.91	4384	1.04	-1.57
scl162-15_	18.36	19.27	4820	1.83	-2.29
scl037tor_	16.43	17.61	4330	0.88	-2.06
scl_11_061	18.89	19.76	4973	2.11	-0.41
SCL2037	17.70	18.76	4504	1.46	-1.57
scl_03_159	18.05	19.11	4520	1.60	-2.22
scl_11_023	16.92	18.03	4428	1.12	-1.92
scl043tor_	17.99	19.17	4296	1.48	-1.16
scl037_20_	18.01	18.93	4798	1.69	-1.24
scl044tor_	18.22	19.17	4725	1.75	-1.73
scl031-14_	17.36	18.31	4737	1.41	-0.89
scl094_06_	17.53	18.54	4606	1.42	-1.97
scl188_11_	18.57	19.47	4839	1.92	-1.86
SCL2036	17.80	18.75	4725	1.58	-1.72
scl_03_018	16.16	17.21	4522	0.85	-1.52
scl071_02_	17.11	18.32	4263	1.12	-1.54
scl052tor_	17.69	18.66	4700	1.52	-2.50
SCL2002	16.03	17.22	4293	0.70	-1.56
scl_02_157	17.30	18.29	4659	1.35	-2.40
scl_11_067	18.50	19.39	4872	1.90	-2.63
scl077tor_	17.36	18.35	4648	1.37	-2.06
scl042_02_	16.62	17.80	4326	0.96	-1.99
scl019_03_	16.37	17.38	4619	0.96	-2.25
scl_03_134	17.34	18.38	4553	1.33	-2.05

Table 4.1 (cont'd)

Name	I (mag)	V (mag)	$T_{eff}$ (K)	log g cgs units	[Fe/H]
scl058-14_	17.03	18.12	4446	1.16	-1.17
scl_03_140	17.73	18.66	4770	1.56	-1.86
scl_11_021	16.26	17.22	4736	0.96	-2.68
scl_03_168	17.52	18.56	4550	1.40	-1.99
scl106_02_	17.77	18.72	4726	1.57	-1.82
scl039_20_	17.89	19.07	4308	1.45	-1.65
scl061tor_	17.93	18.96	4562	1.57	-1.74
scl062tor_	17.12	18.17	4526	1.23	-1.76
scl063_03_	18.13	19.18	4520	1.63	-1.36
scl_14_030	16.50	17.41	4816	1.09	-1.73
scl_03_076	16.53	17.68	4365	0.94	-1.87
scl066tor_	18.52	19.45	4779	1.88	-2.49
scl067tor_	18.69	19.62	4769	1.95	-1.69
scl068tor_	16.87	17.94	4485	1.12	-1.49
scl070tor_	17.24	18.45	4258	1.17	-1.40
scl075tor_	17.04	18.02	4667	1.25	-1.99
scl_03_084	16.80	17.93	4406	1.06	-2.12
scl076tor_	17.48	18.52	4546	1.38	-1.82
scl077tor_	18.02	18.97	4728	1.66	-1.98
scl_03_086	16.92	18.07	4353	1.08	-1.58
scl039-14_	17.09	18.25	4326	1.14	-0.99
scl158_02_	18.25	19.25	4618	1.72	-1.51
scl059_06_	19.10	19.93	5027	2.20	-1.43
scl_11_113	19.22	20.08	4945	2.22	-1.43
scl081tor_	18.40	19.30	4842	1.85	-2.24
scl051tor_	16.88	17.99	4418	1.09	-1.60
scl082_03_	18.60	19.54	4763	1.90	-2.76
scl084tor_	17.89	18.92	4558	1.55	-1.27
scl110tor_	17.81	18.80	4639	1.55	-1.48
scl087tor_	17.29	18.35	4511	1.29	-1.89
scl088tor_	18.05	19.10	4520	1.60	-1.22
scl089tor_	17.51	18.52	4599	1.42	-1.55
scl095_02_	17.48	18.56	4464	1.35	-1.20
scl160-12_	18.34	19.26	4792	1.82	-1.67
scl091tor_	18.20	19.14	4752	1.74	-2.15
scl100_02_	17.58	18.64	4512	1.41	-1.93
scl092tor_	17.51	18.47	4708	1.45	-2.03
scl093tor_	18.87	19.82	4725	2.01	-1.63
scl_02_150	17.93	18.9	4692	1.62	-2.25
scl_11_042	17.46	18.6	4362	1.3	-1.32
scl_02_549	19.67	20.52	4985	2.42	-1.11
scl043_03_	18.00	19.04	4554	1.59	-2.17
scl097tor_	18.20	19.20	4638	1.70	-2.52
scl043tor_	16.33	17.83	3939	0.66	-1.44
scl016_02_	16.27	17.26	4644	0.93	-1.85
scl045-14_	18.46	19.29	5147	2.01	0.10
scl_02_144	17.71	18.66	4725	1.54	-1.45
scl148tor_	18.25	19.16	4816	1.79	-1.84
scl_03_175	18.04	18.99	4745	1.67	-2.69
scl102tor_	18.29	19.21	4792	1.80	-1.81
scl007_08_	16.15	17.26	4416	0.80	-1.48
scl056_02_	17.19	18.06	4917	1.40	-1.42
scl_11_022	16.31	17.45	4395	0.86	-2.17
scl047-14_	15.68	16.98	4197	0.54	-2.30
scl_02_153	18.10	19.09	4653	1.67	-2.34
scl_03_082	16.38	17.35	4687	1.00	-1.94
scl048_03_	19.13	19.98	5051	2.24	-0.19
scl054tor_	16.93	18.02	4459	1.13	-1.85
scl207_02_	18.66	19.58	4792	1.94	-1.78

Table 4.1 (cont'd)

Name	I (mag)	V (mag)	$T_{eff}$ (K)	log g cgs units	[Fe/H]
scl107_03_	19.04	19.94	4840	2.11	-2.03
scl277_02_	19.03	19.95	4792	2.09	-1.83
scl108tor_	17.15	18.22	4498	1.23	-2.00
scl059_25_	17.09	18.13	4555	1.23	-2.09
scl109tor_	17.45	18.48	4564	1.38	-1.78
scl_03_015	16.11	17.31	4275	0.73	-1.47
scl049-14_	16.88	17.95	4500	1.13	-2.05
scl112tor_	17.67	18.85	4300	1.36	-1.33
scl030_20_	17.44	18.74	4133	1.19	-1.23
scl006tor_	15.81	17.08	4177	0.56	-1.38
scl013_20_	16.37	17.48	4420	0.89	-1.68
scl114tor_	18.08	19.05	4691	1.68	-2.23
scl115tor_	18.41	19.41	4624	1.78	-1.96
scl050_09_	16.77	17.86	4456	1.07	-1.75
scl086_02_	17.34	18.44	4451	1.29	-2.09
scl116tor_	17.48	18.55	4495	1.36	-1.93
scl_07_026	16.98	18.06	4464	1.15	-1.26
scl026_02_	16.22	17.47	4239	0.77	-2.10
scl117tor_	18.77	19.69	4796	1.99	-2.25
scl061_08_	19.11	19.95	5107	2.25	0.04
scl_07_018	16.46	17.67	4273	0.87	-1.76
scl116_06_	17.88	18.87	4641	1.58	-1.76
scl175_09_	18.41	19.35	4754	1.84	-1.12
scl119tor_	17.67	18.93	4192	1.31	-1.48
scl120tor_	17.32	18.35	4559	1.33	-1.46
scl_07_055	18.01	18.96	4732	1.66	-2.22
scl015_11_	16.53	17.58	4523	1.00	-1.59
scl_07_025	16.38	17.58	4289	0.84	-1.81
scl051_09_	15.90	16.98	4476	0.73	-1.82
scl122tor_	18.31	19.29	4674	1.76	-2.41
scl130_02_	17.99	19.01	4586	1.60	-1.99
scl053_09_	17.75	18.69	4772	1.57	-2.84
scl_07_130	19.66	20.57	4820	2.36	-1.41
scl034_11_	17.30	18.51	4248	1.18	-0.83
scl198_02_	18.61	19.54	4806	1.94	-0.49
scl124tor_	18.50	19.47	4685	1.84	-1.99
scl055_09_	16.29	17.61	4115	0.73	-1.38
scl144_07_	18.20	19.13	4770	1.75	-1.83
scl125tor_	16.70	17.96	4184	0.92	-1.23
scl050tor_	18.79	19.75	4709	1.96	-2.23
scl040_07_	18.25	19.14	4880	1.82	-1.02
scl147tor_	18.18	19.15	4688	1.71	-2.13
scl126_09_	18.70	19.59	4876	1.98	-2.93
scl_07_021	17.09	18.15	4535	1.22	-2.47
scl072_02_	16.93	18.32	4035	0.94	-1.34
scl029-20_	17.49	18.45	4703	1.45	-1.70
scl012-20_	16.49	17.43	4748	1.06	-1.78
scl131_09_	16.68	17.77	4491	1.04	-2.53
scl_07_041	17.23	18.29	4526	1.28	-2.28
scl040_20_	18.27	19.18	4832	1.81	-0.96
scl057-15_	15.59	16.88	4153	0.46	-1.41
scl_07_128	19.60	20.50	4840	2.34	-1.70
scl058_09_	16.34	17.58	4257	0.82	-2.18
scl059-14_	16.44	17.68	4218	0.83	-1.42
scl017-14_	16.27	17.65	4051	0.69	-1.43
scl_07_051	17.62	18.81	4296	1.34	-1.70
scl135_08_	17.97	19.06	4454	1.54	-1.73
scl_07_056	18.13	19.06	4782	1.72	-2.53
scl_07_022	17.00	18.15	4350	1.11	-1.49

Table 4.1 (cont'd)

Name	I (mag)	V (mag)	$T_{eff}$ (K)	log g cgs units	[Fe/H]
scl_07_023	16.42	17.45	4561	0.97	-1.59
scl_07_121	19.08	19.98	4840	2.12	-2.11
scl140_07_	18.09	19.08	4655	1.66	-2.38
scl_07_024	16.34	17.64	4143	0.76	-1.46
scl141_09_	18.74	19.66	4798	1.97	-2.37
scl142_09_	17.96	18.93	4684	1.63	-1.90
scl143_09_	18.19	19.11	4793	1.75	-1.96
scl144_07_	16.84	18.01	4328	1.04	-1.73
scl145_07_	18.30	19.30	4625	1.75	-0.91
scl_07_007	16.21	17.66	3981	0.63	-1.40
scl146_09_	17.38	18.33	4727	1.41	-1.88
scl334_04_	19.25	20.15	4863	2.21	-0.86
scl148_07_	18.04	19.01	4681	1.66	-1.64
scl_07_043	17.43	18.50	4493	1.34	-1.87
scl015-17_	15.95	17.20	4211	0.64	-1.58
scl118_07_	17.83	18.90	4488	1.50	-1.70
scl_07_129	19.55	20.42	4938	2.36	-0.95
scl151_09_	17.55	18.59	4543	1.41	-1.70
scl028-12_	17.05	18.20	4347	1.13	-1.33
scl041_11_	18.37	19.28	4830	1.83	-2.77
scl_07_057	18.12	19.11	4639	1.67	-1.60
scl037-12_	17.90	18.85	4741	1.62	-2.53
scl_07_144	19.39	20.24	4975	2.30	-1.36
scl_07_019	16.73	17.89	4351	1.01	-1.92
scl049-12_	18.55	19.53	4670	1.87	-0.88
scl040_07_	16.56	17.77	4293	0.92	-2.15
scl063_09_	17.05	17.91	4941	1.35	-1.50
scl064_09_	16.84	17.99	4344	1.05	-1.14
scl065_09_	18.76	19.64	4901	2.03	-1.15
scl066_09_	18.08	18.98	4892	1.76	-0.37
scl009-12_	16.26	17.30	4542	0.89	-1.62
scl035_08_	16.56	17.62	4505	1.00	-1.58
scl_07_086	18.28	19.27	4645	1.74	-2.04
scl067_09_	16.34	17.72	4048	0.71	-1.37
scl_07_150	19.01	19.99	4661	2.04	-1.32
scl020-12_	16.70	17.77	4504	1.06	-2.11
scl_07_017	16.24	17.48	4252	0.78	-2.10
scl_07_103	19.07	19.97	4855	2.14	-1.03
scl_07_059	17.60	18.50	4840	1.54	-1.58
scl082_08_	17.30	18.40	4434	1.27	-1.58
scl_07_037	17.48	18.42	4757	1.46	-2.29
scl068-15_	17.25	18.19	4762	1.37	-2.43
scl_07_048	17.97	18.96	4648	1.61	-2.14
scl071_09_	18.98	19.83	5045	2.18	-0.25
scl010-12_	16.11	17.32	4271	0.73	-1.72
scl027tor_	17.31	18.42	4413	1.26	-1.40
scl165_07_	17.71	18.62	4816	1.57	-1.68
scl057-17_	17.21	18.12	4823	1.37	-2.29
scl_07_138	19.17	20.04	4959	2.22	-0.60
scl073_09_	18.63	19.55	4802	1.93	-2.59
scl167_09_	18.09	18.94	4970	1.76	-2.62
scl_07_044	17.64	18.52	4895	1.57	-1.31
scl_07_089	18.97	19.85	4910	2.12	-0.95
scl018_08_	16.74	17.71	4684	1.14	-1.84
scl_07_046	17.78	18.81	4574	1.51	-2.19
scl033tor_	16.21	17.59	4038	0.65	-1.15
scl_07_093	18.91	19.90	4640	1.99	-1.29
scl343_06_	19.26	20.17	4816	2.19	-1.69
scl_07_001	15.83	17.10	4204	0.59	-1.91

Table 4.1 (cont'd)

Name	I (mag)	V (mag)	$T_{eff}$ (K)	log g cgs units	[Fe/H]
scl_07_083	18.97	19.87	4840	2.08	-1.67
scl043-12_	18.48	19.37	4870	1.89	-2.52
scl_07_126	19.37	20.29	4810	2.24	-0.91
scl174_07_	17.69	18.65	4725	1.53	-2.64
scl_07_006	15.60	17.11	3935	0.37	-1.48
scl175_09_	16.20	17.14	4760	0.95	-2.28
scl_07_075	18.38	19.3	4799	1.84	-1.20
scl028-13_	17.47	18.49	4578	1.39	-1.30
scl241-10_	18.90	19.82	4792	2.04	-1.83
scl022_05_	16.70	17.92	4255	0.96	-1.68
scl011-12_	16.05	17.34	4159	0.65	-1.55
scl008_11_	16.21	17.31	4433	0.83	-1.50
scl025_09_	17.07	18.08	4599	1.24	-1.54
scl_07_120	19.02	19.91	4880	2.13	-1.04
scl040_25_	18.07	18.97	4846	1.72	-2.41
scl181_07_	18.50	19.34	5001	1.95	-1.32
scl_07_053	17.92	18.78	4953	1.71	-1.14
scl030_04_	17.75	18.82	4483	1.47	-0.98
scl030tor_	17.67	18.62	4738	1.53	-2.38
scl014-15_	16.75	17.66	4816	1.19	-1.56
scl186_08_	18.39	19.46	4488	1.73	-1.73
scl_07_045	17.84	18.73	4866	1.64	-1.45
scl048tor_	18.03	19.05	4581	1.62	-1.72
scl004_08_	15.64	16.92	4171	0.49	-1.54
scl_07_015	16.36	17.55	4288	0.83	-1.41
scl033_08_	17.93	19.09	4329	1.48	-1.28
scl_07_151	19.17	20.03	4950	2.21	-1.28
scl002_09_	15.73	16.84	4416	0.63	-1.52
scl034_06_	18.06	19.13	4485	1.59	-1.55
scl001_06_	15.90	17.06	4339	0.67	-1.60
scl053tor_	18.28	19.38	4428	1.66	-1.11
scl046_09_	18.59	19.42	5074	2.02	-0.58
scl_07_111	19.61	20.52	4846	2.35	-0.71
scl053_07_	18.32	19.38	4504	1.71	-0.86
scl001_07_	15.69	16.94	4222	0.54	-1.78
scl_07_066	17.97	18.94	4682	1.63	-1.31
scl026_09_	16.76	18.11	4081	0.90	-1.39
scl_07_067	18.05	19.09	4540	1.61	-1.55
scl044-15_	17.73	18.90	4315	1.39	-1.35
scl004-15_	16.16	17.08	4793	0.95	-1.48
scl002_25_	15.61	16.93	4155	0.49	-2.03
scl039tor_	18.05	18.96	4819	1.71	-1.38
scl017-12_	16.11	17.61	3925	0.55	-1.21
scl034tor_	17.21	18.40	4286	1.17	-1.36
scl022tor_	17.21	18.05	4994	1.43	-1.50
scl026_07_	17.14	18.09	4725	1.31	-1.57
scl017tor_	16.67	17.60	4770	1.14	-1.43
scl018_08_	16.65	17.98	4101	0.86	-1.34
scl038tor_	17.83	18.94	4415	1.47	-1.50
scl_07_032	17.05	18.47	4005	0.98	-1.35
scl036_09_	17.66	18.51	4970	1.61	-1.42
scl051_03_	18.36	19.28	4796	1.83	-1.36
scl008_08_	16.20	17.10	4839	0.98	-1.79
scl004_07_	15.70	16.99	4165	0.52	-1.65
scl050-20_	18.65	19.58	4773	1.94	-1.29
scl054-10_	19.07	20.01	4747	2.09	-1.71
scl042tor_	17.90	19.03	4381	1.49	-1.50
scl035_20_	17.88	18.84	4708	1.61	-1.11
scl014_08_	16.43	17.70	4171	0.81	-1.23

Table 4.1 (cont'd)

Name	I (mag)	V (mag)	$T_{eff}$ (K)	log g cgs units	[Fe/H]
scl043_25_	18.11	19.05	4755	1.72	-1.06
scl029-17_	17.48	18.61	4393	1.33	-1.88
scl032-15_	17.47	18.76	4151	1.21	-1.39
scl028_09_	17.20	18.16	4711	1.33	-2.10
scl031_07_	17.41	18.39	4661	1.40	-1.27
scl016-15_	16.40	17.58	4314	0.86	-1.73
scl014_09_	16.45	17.40	4728	1.04	-1.88
scl032_08_	18.05	19.05	4621	1.64	-1.75
scl023_08_	17.01	18.26	4201	1.05	-1.34
scl032_07_	17.43	18.41	4664	1.41	-1.87
scl055tor_	19.13	20.06	4770	2.12	-1.98
scl037_09_	17.62	18.54	4793	1.53	-1.51
scl022_04_	17.04	18.17	4380	1.14	-1.40
scl071tor_	19.31	20.16	4978	2.27	-1.26
scl031_08_	18.17	19.00	5092	1.87	-0.38
scl020_32_	16.92	18.02	4430	1.11	-1.37
scl025-17_	17.03	18.07	4539	1.20	-1.25
scl052_05_	18.41	19.33	4798	1.85	-1.27
scl040_07_	17.88	18.83	4726	1.61	-1.36
scl012-15_	16.33	17.59	4224	0.80	-2.05
scl015_09_	16.82	17.72	4839	1.22	-1.69
scl029tor_	17.06	18.24	4306	1.12	-1.55
scl047tor_	18.02	19.03	4600	1.62	-1.13
scl045_07_	18.04	19.06	4580	1.62	-1.10
scl017_04_	16.46	17.96	3942	0.71	-1.49
scl020-12_	16.79	18.15	4074	0.91	-1.48
scl010_08_	16.18	17.38	4309	0.78	-2.16
scl018-10_	16.14	17.64	3931	0.57	-1.31
scl029_32_	17.25	18.26	4611	1.31	-2.10
scl030_32_	17.12	18.33	4262	1.13	-1.51
scl005_09_	16.20	17.13	4771	0.96	-1.35
scl049_11_	18.08	19.07	4639	1.66	-1.50
scl005_32_	16.04	16.99	4725	0.87	-1.61
scl010_32_	16.28	17.41	4383	0.84	-1.52
scl016tor_	16.61	17.57	4703	1.09	-1.67
scl054-12_	18.49	19.42	4774	1.87	-1.26
scl023_09_	16.87	17.85	4664	1.18	-1.85
scl045_09_	17.99	18.94	4740	1.67	-0.81
scl037_09_	17.52	18.69	4312	1.30	-1.15
scl010_09_	16.39	17.36	4681	1.00	-1.54
scl027_32_	16.96	18.18	4247	1.05	-1.48
scl039_32_	17.95	18.82	4920	1.69	-2.56

Table 4.2. CEMP candidates in Sculptor

Name	$T_{eff}$ (K)	log g cgs units	[Fe/H]	Comments
scl_03_110	4415	1.23	-1.45	
scl081_02_	4245	0.92	-1.71	
scl055_11_034	4259	1.36	-1.40	
scl084tor_	4343	1.20	-1.69	
scl036_06_	3966	0.50	-1.42	
scl076_02_	4304	0.82	-2.67	carbon star (Azzopardi et al. 1986)
scl092tor_	4465	1.32	-1.94	
scl094tor_	4085	0.75	-2.92	carbon star (Azzopardi et al. 1986)
scl_14_012	4330	0.80	-1.72	